AD_____

Award Number: W81XWH-10-1-0774

TITLE: Theory-Driven Models for Correcting “Fight or Flight” Imbalance in Gulf War Illness

PRINCIPAL INVESTIGATOR: Gordon Broderick, Ph.D.

CONTRACTING ORGANIZATION: University of Alberta
Edmonton, Alberta, Canada, T6G 2C8

REPORT DATE: September 2013

TYPE OF REPORT: Final

PREPARED FOR: U.S. Army Medical Research and Materiel Command
Fort Detrick, Maryland 21702-5012

REPORT DOCUMENTATION PAGE

Form Approved
OMB No. 0704-0188

1. REPORT DATE	2. REPORT TYPE	3. DATES COVERED
September 2013	Final	1 September 2010 – 31 August 2013

4. TITLE AND SUBTITLE

Theory-Driven Models for Correcting "Fight or Flight" Imbalance in Gulf War Illness

5a. CONTRACT NUMBER

5b. GRANT NUMBER
W81XWH-10-1-0774

5c. PROGRAM ELEMENT NUMBER

6. AUTHOR(S)

Gordon Broderick, Ph.D.

E-Mail: gordon.broderick@ualberta.ca

5d. PROJECT NUMBER

5e. TASK NUMBER

5f. WORK UNIT NUMBER

7. PERFORMING ORGANIZATION NAME(S) AND ADDRESS(ES)

University of Alberta
Edmonton, Alberta, Canada, T6G 2C8

8. PERFORMING ORGANIZATION REPORT NUMBER

9. SPONSORING / MONITORING AGENCY NAME(S) AND ADDRESS(ES)
U.S. Army Medical Research and Materiel Command
Fort Detrick, Maryland 21702-5012

10. SPONSOR/MONITOR'S ACRONYM(S)

11. SPONSOR/MONITOR'S REPORT NUMBER(S)

12. DISTRIBUTION / AVAILABILITY STATEMENT
Approved for Public Release; Distribution Unlimited

13. SUPPLEMENTARY NOTES

14. ABSTRACT

The objective of this study is to create a comprehensive engineering model of endocrine-immune interaction dynamics in order to identify (i) theoretical failure modes of the HPA-immune axis that align with GWI, and (ii) promising treatment strategies that exploit the regulatory dynamics of these systems to reset control of the HPA-immune axis to normal.

We are currently transferring operations and this award to Nova Southeastern University, FL, to facilitate interactions with U.S. sponsors and collaborators. Dr. Craddock, now assistant professor at Nova, will continue in his role on this project. Work has focused on the refinement of the HPA-HPG-immune multi-axis model, its validation scheme and inclusion of Th17 and neurotranmission (NPY, acetylcholine, etc…)in the detailed immune model. Importantly we have developed an advanced prototype of a neuroinflammation model. Deployment to large-scale distributed computing platform has also advanced significantly.

15. SUBJECT TERMS
GWI; Hypothalamic-pituitary-adrenal (HPA) axis

16. SECURITY CLASSIFICATION OF:			17. LIMITATION OF ABSTRACT	18. NUMBER OF PAGES	19a. NAME OF RESPONSIBLE PERSON
					USAMRMC
a. REPORT	b. ABSTRACT	c. THIS PAGE			19b. TELEPHONE NUMBER *(include area code)*
U	U	U	UU	56	

Table of Contents

Introduction

The hypothalamic-pituitary-adrenal (HPA) axis controls the body's "fight or flight" response through a series of endocrine and immune signals directed at ensuring immediate survival and later re-establishing homeostasis. Changes in the tone of this response have been observed in veterans with Gulf War Illness (GWI). Studies report abnormal cell proliferation, impaired function and persistent oxidative stress in circulating immune cells of patients. Similarly dysregulation of the HPA axis includes hypersensitivity in cytokine feedback as well as suppression of cortisol and neurotransmitters responsible for mediating innate and adaptive immunity. This is further complicated by the impact on the HPA axis of a myriad of regulatory interactions both within and between i) the immune system and ii) the sex-hormone axis, the hypothalamic-pituitary-gonadal (HPG) axis.

We proposed that severe physical or psychological insult to the endocrine and immune systems can displace these from a normal regulatory equilibrium into a compromised stable state. This state is characterized by a self-perpetuating inflammatory response that involves regulatory imbalance between the HPA, HPG and immune axes. To explore the validity of this hypothesis our objective was to create comprehensive engineering models of endocrine-immune interaction dynamics in order to identify (i) theoretical failure modes of the endocrine-immune interplay that align with GWI, and (ii) promising treatment strategies that exploit the naturally occurring stable points of these systems.

Body.

At the time of our last update we had completed a re-assessment of the modeling approach and successfully identified, refined and deployed a discrete modeling paradigm enabling us to circumvent the significant gaps in the required parameter estimates exist in the literature. This new approach was described in greater detail in the previous report (September, 2012) (**Task 1**) and consists in an extension of the discrete logical network methodology proposed originally by Thomas et al. [1,2] and developed further by Mendoza and Xenarios [3]. *Importantly, this approach supports the seamless integration of kinetic information wherever available, be it simple sequential precedence, relative time scale or detailed dynamics*.

We have now *completed* the original scope of Task 1 through Task 5. However as a result of improvements in computational efficiency we have been able to extend the basic models beyond what was originally anticipated. With the concerted efforts of Dr. Craddock, new programming staff Mark Rice and Ryan del Rosario and research interns Simar Singh and Lundy McKibbin we have continued to: *(1) design and deploy a distributed version of the computing code, (2) increase the granularity of the multi-axis model and the implement a statistical scheme for model validation, (3) significantly extend the scope and increase fidelity of the detailed immune model, and (4) develop a prototype model of neuro-inflammation, and (5) designed and deployed a first prototype of the treatment optimization scheme*.

*1. Continued algorithm development and speed-up. (**Task 1**)*. The core concept of the approach we have used is *connectivity*. Key biological regulatory processes have been translated into a set of discrete logic circuits. Analysis of these networks makes it possible to identify the number and type (e.g. oscillatory, etc…) of resting states as well as their molecular and cellular profile without detailed knowledge of response dynamics. Early implementations of this analysis were made in a high-level rapid-prototyping environment (Python) facilitating development but severely limiting computational performance. As mentioned previously, under this discrete formalism the number of model variables determines the total number of system-wide states such that a model of N state variables possesses 3^N states. As a result the number of total system-wide states increases rapidly as new state variable elements are added. Initially these calculations were encoded into a rapid-prototyping Python script that was used to search the above-mentioned network for stable equilibrium states (Version 0). Within a 24-hour threshold time (86,400 seconds) this version is capable of analyzing up to 14 variables (4,782,969 states) with a memory usage in the range of gigabytes (GB) (**Figure 1**). High-performance computing staff, programmers Rice and del Rosario, re-engineered the search algorithm and its implementation in several stages. First, the algorithm was directly re-coded in the C programming language (Version 1) as it is both memory-efficient and approximately 30 times faster than

Python. This increased performance enabled analysis of a 17-variable model (129,140,163 possible discrete states) in 24 hours at a memory usage in the megabyte (MB) range. Next, the serial algorithm was re-engineered through the introduction of ternary data structures to efficiently optimize memory usage and run time, and prepare the algorithm for parallel implementation (Version 2). Here, in the 24-hour threshold time, a 19-variable model (1,162,261,467 states) was analyzed at MB memory usage. Thirdly, the algorithm was implemented with parallel tasking (Version 3), using multiple levels of parallel threading (m0 to m4). Here we have successfully run a model with 23 variables (94,143,178,827 states) within a day using only MB's of memory. Finally, we have parallelized the code further with a supervisory layer based on message passing interface (MPI) (Version 4) to make full use of the high-performance computing resources on the University of Miami's Pegasus cluster. While performance measures are still being evaluated we have successfully analyzed a 25 variable circuit model (847,288,609,443 discrete states). Continued improvements to computational efficiency are ongoing.

2. *Continued refinement of an integrated model of HPA-HPG-immune interaction (**Task 3, Task 5**)*. We had previously extended our early model of HPA axis dynamics [4] by including feed-forward and feedback interactions with sex hormone regulation and immune response. A circuit model had been constructed that linked state variables across the HPA axis with hypothalamic-pituitary-gonadal (HPG) function in both men and women, as well as a coarse-grained mode of the immune system consisting of innate (IIR) and adaptive (AIR) immune components. A critical review of this model prompted us to: (i) re-assess the coarse-graining of the immune components (IIR and AIR aggregate nodes), increasing the level of detail to improve fidelity, and (ii) define and implement an alternate validation measure.

- *A modified multi-axis model*. In a first coarse iteration of the model, immune function was described simply in terms cytokine activity of the innate (IIR) and adaptive (AIR) immune responses. Here the aggregation of all adaptive immune response into the AIR node lacked the complexity needed to capture shifts between Th1 and Th2 activity. Further resolution was added to the immune model by separating the AIR into Th1 and Th2 activity and by adding both cell population activity, as well as cytokine signaling separately. In this modified immune module innate immune cells (ICells) produce cytokines that regulate the innate immune response (IIR) including interleukin (IL) -1, IL-6, IL-8, IL-12, IL-15, IL-23 and tumor necrosis factor alpha (TNF-α). These IIR signals serve to prime helper T cells towards a Th1 type adaptive immune response (T1Cell), producing Th1 pro-inflammatory cytokines (T1Cyt) including IL-2, interferon-gamma (IFN-γ), and tumor necrosis factor beta (TNF-β). This further activates ICells, while suppressing the Th2 adaptive immune response (T2Cell). The T2Cell node promotes the production of the Th2 anti-inflammatory cytokines (T2Cyt) IL-4, IL-5, IL-10 and IL-13, which serve to inhibit the activity of T1Cell and ICells. Interaction with the HPA axis is mediated by CORT suppressing ICell and Th1Cell activity, while IIR and Th1Cyt signals stimulate the HPA. Additionally, new interactions between the immune and HPG axis were included where Th1Cyt signals suppress GnRH and LH/FSH release and the dimorphic response of sex hormones TEST/ EST serve to induce Th1/Th2 activity.

- *A probabilistic measure of alignment with experimental data*. Alignment of model predictions with experimental data were previously assessed on the basis of discrete Hamming distance and visualized with a Sammon projection of the latter. In order to provide a more continuous measure of similarity or dissimilarity we have adopted a probabilistic measure proposed by Brown [5]. Here, we calculate the significance of alignment between experimental data and a given state predicted by the model using a meta-analysis technique that combines non-independent test statistics. Null probability p-values for individual variables are calculated using two-sample t-tests between ill subjects and healthy controls. To give the probability of obtaining the model value by chance 'right-handed' one-tailed tests are used when the model predicts a high state, 'left-handed' tests when predictions are low, and two-tailed tests when the prediction is a nominal value. These non-independent statistics are then combined into a chi-squared test statistic, which is scaled to $T = T_0/c$ with 2N/c degrees of freedom, where $c = \sigma^2/4N$. This statistic is then used in the scaled chi-squared distribution to determine the overall probability of obtaining the alignment by chance. The advantage of this method is that it accommodates for the dependence between variables, allows for a statement of confidence on alignment for each individual

model predicted state, and does not depend on the number of measureable markers allowing for direct comparison across models.

Details of this analysis and the final multi-axis model are described in Appendix A in manuscript recently submitted to PLoS One [6]. In brief, co-regulation of the HPA, HPG and immune systems has been described as a revised circuit model consisting of 14 state variables where each variable can assume one of three discrete states at any point in time: -1 (inhibited), 0 (nominal) and +1 (elevated). In this model the HPA axis continues to be described in terms of corticotropin-releasing hormone (CRH), adrenocorticotropic hormone (ACTH), cortisol (CORT) and cytostolic glucocorticoid receptors (GRs), which unlike membrane bound receptors, dimerize (GRD) (**Figure 2A-B**). HPG function is again described by the levels of gonadotropin-releasing hormone (GnRH), of luteinizing homone (LH) as well as testosterone (TEST) in males (**Figure 2 C**) and estradiol (EST) in females (**Figure 2 D-G**). As before, the effects of gender merit special attention as testosterone (TEST) exhibits an inhibitory effect on the HPA axis while estrogen (EST) and progesterone can stimulate or suppress HPA activity depending on the phase of menstrual cycle. Theses components are integrated with the revised immune model described above.

Results of simulations conducted on the refined model can be summarized as follows:

- *Male subjects*. Inclusion of basic immune function and sex hormone regulation by the HPG axis with HPA function (HPA-GR-Immune-HPG model) *in male subjects* (**Figure 2C**) resulted in the emergence of 5 stable equilibrium states. Once again the first state was that of normal health (SS0). Low levels of ACTH and elevated expression of the glucocorticoid receptors GR and GRD characterized the second equilibrium state (SS1). The third stable state (SS2) exhibited supprssed innate and Th1 immune responses (low ICell, IIR, T1Cell, and T1Cyt), with increased Th2 activity (high T2Cell and T2Cyt). The fourth state (SS3) presented low ACTH, suppressed innate and Th1 immune activity (low ICell, IIR, T1Cell and T1Cyt), and elevated Th2 and glucocorticoid receptor activity (high GRD, GR, T2Cell and T2Cyt). The final state (SS4) displayed hypercortisolism, suppressed HPG activity and a shift towards the Th1 immune response (low T2Cell, T2Cyt, GnRH, LH/FSH and TEST/EST, and high CORT, GRD, GR, T1Cyt and T1Cell).
- *Female subjects*. In the specific case of positive feedback along the HPG axis and suppressive interaction with the HPA axis, the HPA-GR-Immune-HPG model for female subjects (**Figure 2F**) supported 11 steady states. In addition to 5 states equivalent to those obtained for the male subjects, we found new steady states that corresponded to suppressed HPA axis and innate immune response (low CRH, ACTH, CORT, ICell and IIR), while the HPG and anti-inflammatory response were elevated (high T2Cell, T2Cyt, GnRH, LH/FSH and EST). This combination occurred at each of the three low, nominal and high values for glucocorticoid receptor activity (GR/GRD) (SS5, SS6 and SS7, respectively). The final three additional states all supported suppressed HPA (CRH, ACTH, and CORT) and T1Cell activity, with elevated HPG activity (GnRH, LH/FSH and EST). These were again differentiated by their glucocorticoid receptor levels (GR/GRD at low (SS8), nominal (SS9) and high (SS10) values). Note that a stable steady state characterized by low cortisol levels was found *only for female subjects*.
- *Alignment with experimental data*. To validate these results the predicted steady states were first compared to steroid and cytokine levels recorded in male Gulf War veterans with GWI and healthy veterans (HCs) as part of a sister study [7]. As experimental measures for ACTH, GR, GRD, and immune cells populations were not available, certain steady states could not be distinguished and validated separately from one another. Comparison to the nominal states (SS0/SS1) showed poor alignment, with a null probability of p=0.82, suggesting that the GWI profile cannot be considered the same as normal behavior. The predicted states presenting a shift towards Th2 immune activation (SS2/SS3) showed improved alignment with a significance of p=0.38. However the final state (SS4) displaying hyper-cortisolism, low TEST and a shift towards Th1 immune activation yielded the best alignment with a null probability of p=0.30, supporting the notion of a more classical Th1 auto-immune signature with a concurrent (and perhaps stabilizing) endocrine component in GWI.

  As a much greater proportion of women than men are affected by CFS, we compared the predicted steady states identified with the female model to experimental data collected under two compatible

studies [8,9]. Alignment with the baseline nominal setting in measureable variables (SS0/SS1) was poor, p=0.83, reinforcing that CFS is distinctly different from normal regulatory behavior. The Th2-shifted immune profiles predicted by the model (SS2/SS3) showed a significant alignment with the measured signature (p=0.04), suggesting that Th2 activation in CFS may at least in part be supported by homeostatic drive. This emphasized further by a low degree of alignment with the Th1 immune activated state, with hypercortisolism, and low EST (p=0.28). Improved alignment was found with states with a shift towards Th2, coupled with hypocortisolism, and high EST (SS5/SS6/SS7) (p=0.02). States presenting with only hypocortisolism and high EST, and no immune activation (SS8/SS9/SS10) aligned very weakly with the measured profile (p=0.60), suggesting that hypocortisolism, increased EST, and Th2 activation in combination are key CFS profile features that might owe at least part of their persistence to basic homeostatic control.

*3. Refinement of detailed immune circuitry including Th17 and neurotransmission (**Task 2, 3 and 5**).* Based on the work of Folcik et al. (2007, 2011) [10,11] and an extensive review of recent literature, we constructed an initial wiring diagram describing cytokine signaling between immune cell populations [12] (see excerpts of manuscript in preparation; Appendix B in 2012 annual report). We have now extended this first detailed model of immune signaling at two levels of granularity:

- *Addition of Treg and Th17 components to aggregate model of cytokine signaling.* The specific cytokines supported in the initial model included interleukin (IL)-1, IL-2, IL-4, IL-5, IL-6, IL-8, IL-10, IL-12, IL-13, IL-23, IL-27, interferon (IFN)-γ, and tumor necrosis factor (TNF)-α. In order to improve computational efficiency, cytokines were grouped according to their dominant action into either a monokine (MK) or cytokine (CK) group (Folcik et al., 2011)[11]. We have now extended the model to include the actions of IL-17, 21 and 23 as well as TGF-β. The extended model also includes T regulatory (Treg), Th17 and activated Th17(23) cell populations as well as IgA and IgG antibody classes. This updated version of the cytokine signaling network includes as before the effects of stress and sex hormones for male subjects only at this time (**Figure 3**). Results of our stability analysis on this second-generation model that can be summarized as follows:

    - *Stable immune response modes in male subjects*. Application of this discrete dynamical analysis to the detailed endocrine-immune network yielded three predicted stable steady states. As always, the first state was that of normal health (SS0). The second stable state (SS1) presented with low anti-inflammatory cytokines (CK2), low testosterone, and suppressed NK cell activity, Th1 and Th2 immune cell activity, accompanied by elevated Th1 inflammatory cytokines (CK1), high cortisol levels, and increased cytotoxic T lymphocyte (CTL) and Treg cell activity. The third stable attractor (SS2) also displayed low NK cell activity and testosterone levels, with elevated cortisol, CK1 and CTL activity. However this state presented a different immune profile characterized by low TGF-β levels, elevated monocyte cytokines (MK1, MK2, MK6, MK21), and increased Th17 activity (CK17, Th17(23), TH17b). These results are consistent with the findings of the integrated HPA-HPG-immune model discussed above, but with added resolution in terms of immune function, which indicates alternate equilibria defined by different stable levels of regulatory T cell activity, or Th17 immune response.

    - *Alignment with experimental data*. Once again, these predicted steady states were compared with experimental data used in Section 1 [7-9]. We found alignment of GWI with the healthy reference state (SS0) corresponded to a null probability of p=0.87, indicating very poor alignment. Improved alignment was observed with SS1 (p= 0.30). This is comparable to the results found for the high CORT, low TEST, elevated Th1 response state using the integrated HPA-HPG-Immune model described previously (section 2). Further improvement was found when comparing GWI to the final predicted stable state (SS2) (p=0.12), suggesting that chronic Th17 activation, hypercortisolism, and low TEST observed in this illness may persist in part as a result of homeostatic drive. For male CFS subjects we found comparably poor alignment with the reference baseline state SS0 (p=0.76). However, alignment with state SS1 (p=0.16) was dramatically different from GWI, emphasizing the distinct nature of CFS. Distinct as they may be, these illnesses nonetheless share some common components that our group has begun to

delineate at the level of specific pathways [13]. Consistent with this we found comparable alignment of CFS and GWI with SS2 (p=0.12) albeit for slightly different reasons. Thus, while GWI aligns best with Th17 dysregulation, CFS alignment suggests slightly different imbalance of Th17 and/or Treg response.

.

- *High fidelity model of individual cytokine actions.* Improved alignment with the clinical data can be accomplished by including additional key interactions in the model regulatory network, and by increasing resolution of the model in terms of the state variables represented. Key interactions located outside the immune network include critical neurotransmitters linking the brain and central nervous system with the HPA axis and the immune system. The neurotransmitters norepinephrine (NorEpi), and acetylcholine (ACh) are significant regulators of cytokine production, and therefore immune function. Neuropeptide Y (NPY) is also key component of the stress response, and its subsequent effects on the immune system. The latter has now been shown to play a significant role in CFS [14]. These messengers have now been included in a more refined model of the immune system and it's interface with neurotranmission (**Figure 4**). Their effect on the immune system however is not simple. In the previous immune model several cytokines were aggregated into groups. NorEpi, ACh and NPY were found to have differing effects on the production of cytokines within individual groups. To accommodate these varied responses several of the aggregate nodes were separated into their individual constituent entities increasing the resolution, and complexity, of the extended immune model. The overall resulting high fidelity model of the extended immune system, including HPA, HPG and CNS inputs is shown in **Figure 4**. A first analysis has shown the following:

    - *Preliminary stable immune response modes in male subjects*. Discrete logical analysis of the preliminary high fidelity extended immune model produced two steady states. Normal health characterized the first state (SS0), while the second state (SS1) presented with low IL-1, MK6, TEST and NK cell activity, and high IL-12, MK2, CK1, CK2, CTL, CORT and NPY. Note that several of the cytokines that were once aggregated (IL-1, IL-8, IL-12) now present with differing profiles. These yield a complicated mixed Th1:Th2 profile consistent with our previous analysis of GWI. Further refinement of other aggregate nodes, and inclusion of the Th17 axis is currently underway.

    - *Preliminary alignment with experimental data*. We found in GWI that aligns with the nominal steady state (SS0) at a significance level p=0.85 again indicating poor alignment with normal health. Alignment with the alternate steady state (SS1) however was much more significant (p= 0.07). This both supports a notion of a complex stable combined Th1:Th2 response in this illness, and suggests a brain component in its perpetuation. Further analysis with the refined model is being conducted.

Collectively these simulations of known endocrine-immune circuitry support the existence alternate homeostatic regimes, some of which overlap substantially with observed immune and endocrine status in male GWI and female CFS subjects. Such overlap with naturally occurring stable regulatory regimes would certainly be consistent with the persistence of symptoms long after the initiating event. This same characteristic may also explain why these illnesses appear in many ways resistant to treatment.

*4. An early model of neuroinflammation (extension to **Task 3**)*. Elevated levels of pro-inflammatory cytokines negatively impact learning, memory and neurogenesis. The intense immune activation in the brain that characterizes infections, injury, neurotrauma and severe/chronic stressful conditions, can induce hyper-excitability of neuronal circuits perpetuating an inflammatory state within the CNS resulting in excitotoxicity, and eventually apoptosis and neurodegeneration resulting in learning and memory impairments. To explore these mechanisms we have constructed a first model with Neurons, Neural Progenitor Cells (NPCs), Endothelial Cells (ECells), Microglia, and Astrocytes as key cellular components, while interleukin (IL)-1, IL-4, IL-6, tumor necrosis factor (TNF)-α, and OX-2 membrane glycoprotein (CD200) comprise a simplified neuro-inflammatory response. As numerous studies show communication of inflammatory information to the brain via both humoral and neuronal mechanisms, hormone signaling is included via Insulin-like Growth Factor 1 (IGF-1), Vascular Endothelial Growth Factor (VEGF), Brain Derived

Neurotrophic Factor (BDNF), and cortisol (CORT). The neurotransmission component is conveyed with the inclusion of Acetylcholine (ACh), Norepinephrine (NE), Glutamate (Glut), and Adenosine Triphosphate (ATP). Stress-induced immune activation is a neurally initiated phenomenon, via the activation of noradreneregic pathways and altered cholinergic neurotransmission. Elevated brain cytokines produce further activation of stress response systems such as the HPA axis and the SNS. The multiple feed forward and feedback connections between these elements found in the neurophysiology literature are depicted in the circuit model shown in **Figure 5**.

- *Stable immune response modes in the brain - a first analysis:* Interaction among these various cell populations via immune, hormone and neurotransmitter signals ultimately revealed two steady states. The first, again, is the normal reference state of health (SS0). The alternate steady state (SS1) is characterized by low levels of ACh, BDNF, IGF-1, IL-4, and VEGF and suppressed activity of Astrocytes, ECells, NPCs, and Neurons, accompanied by elevated levels of CORT, Glut, IL-1, IL-6, and TNF-α, and over activation of Microglia. This is consistent with a chronic neuroinflammatory state. The elevated CORT levels, seen to align with GWI in our other models, suggests a possible involvement of a persistent and stable neuro-inflammatory cascade in this illness.

*5. Continued development of treatment design (**Task 6, 7**)*. Analysis of the above-mentioned regulatory signaling circuits not only provides information describing the stable steady states available to the system but also extensively describes the ensemble of transitory states that lead *unequivocally* to one steady state or another; these are said to lie within that steady state's *basin of attraction*. Importantly, these subsets of transitory states will lead to that specific stable state independently of an individual's immune and endocrine response kinetics. This guaranteed convergence to a healthy equilibrium makes them attractive as broadly applicable treatment destination states. *In the design of minimally invasive interventions our basic paradigm is therefore to identify the closest transitory state(s) that lie within the basin of attraction that ensures a return to normal homeostasis.*

- *A global trajectory search formalism*. We have formalized the treatment course as a vector describing a path from the state of disease to health. Allowable transitions between states along the path consist of normal evolution of the system, as described by our logic rules, and transitions induced by clinically feasible interventions. To find treatment course paths that meet these criteria we have formulated our search as a global optimization problem. We have chosen to use a Genetic Algorithm (GA) optimization method, as the discrete nature of our model naturally accommodates the GA solution procedure. Initially, the GA seeds the solution space by generating random solutions composed of binary strings or "chromosomes" representing a treatment path. Each member of this initial population is checked against a fitness function and assigned a fitness score. Top ranking members of the population are then chosen as the parent solutions for the next generation. Each generation is made up of the chosen parent population plus combinations of crossed-over "mated" parent solutions with a small chance for random mutation. This process runs over a set number of generations or until optimum results are found. This allows a rapid search of the global space, while mutations minimize the chance of remaining in local minima.

- *A multiple objective criterion*. Our fitness function divides the overall the solution string into segments describing each time-step in a treatment course. The overall desirability of a solution is assessed on the basis of three objectives: (i) feasibility or compliance with the model, (ii) compliance with allowable treatment perturbations, and (iii) the minimal invasiveness and duration of treatment. The first and second of these objectives has been implemented in the first trial version. For each time step segment subsequent time-steps are compared to the allowable transition states and assigned a *compliance* score based on the minimum hamming distance separating the proposed solution state and the allowable states. Overall fitness of a solution is then the sum of the hamming measures for all state transitions along a given solution path. A fitness value of zero indicates a perfect compliance with model behavior and allowable interventions.

Based on this paradigm we have started work on **Tasks 6 and 7**. A first fitness function based on model compliance, as well as the GA algorithm itself, have been designed and implemented. Currently, we are in the process of optimizing code parameters (population size, number of generations, mutation rate, etc…) to efficiently search the large state spaces of our multi-systems model.

Additionally, we are currently refining these models as well as the treatment search algorithm to incorporate the effects of timescale. This will make it possible to take advantage of saddle point states or unstable intermediate states that lie between the basins of attraction. We are currently investigating avenues for exploiting broad classes of kinetic scales that might make it possible to reduce the treatment complexity even further and tailor these interventions to patient sub-groups.

6. *Continuing work*. Ongoing work involves the continued refinement of a circuit model describing mechanisms of neuroinflammation and neurotransmission in the brain. Efforts are also now shifting to the completion and validation of the treatment design algorithm. This will be the major area of development as we begin simulation of treatment strategies, the principal deliverable of this project.

Timeline. As described in the previous report dated September 30, 2011, the University of Alberta's Research services Office submitted on behalf of the principal investigator a request for a one-year extension of the project term due to administrative delays. This request was reviewed initially by Ms. Strock and Dr. Phillips of the DoD (January 23, 2012) and we were asked to resubmit this request at a later date (6-8 months before end of project term). We have since confirmed with Dr. Rebecca Fisher that this continues to be the correct course of action (ref. email from Dr. Fisher dated September 21, 2012). In accordance with Dr. Fisher's recommendation we are submitting a formal request for a one-year no-cost extension as part of our request to transfer this award to Nova Southeastern University retroactive to June 1, 2013.

Key Research Accomplishments.
In keeping with the milestones described in the project submission initial efforts were directed at:

- Consistent with the previously completed Task 1, we have further improved the efficiency of the serial C code, again delivering order of magnitude improvements in execution speed and memory usage. Importantly we have engineered a parallel framework based on MPI and Pthread protocols to deploy this code onto distributed high-performance platforms. This code is now deployed and fully operational on the University of Miami Pegasus 2 platform.
- Consistent with the now completed Task 2, we have continued to refine our previous model of immune signaling mechanisms. These now include the actions of Th3 and Th17 axes, implemented in models at two levels of granularity.
- We have now basically completed Task 3 as defined originally. In this regard we have produced a refined multi-axis model, further developed our validation scheme and submitted to PLoS One a first complete manuscript describing co-regulation across HPA, HPG and immune axes in men and women.
- In an extension to original Task 2 and 3, we have produced a first circuit model of inflammatory processes occurring in the brain and involving the cell types and immune signaling specific to this physiological compartment. Early analyses of this model show the persistence of a chronic neuroinflammatory state perpetuated by overactive microglia and underactive astrocytes, leading to loss of neuron function, in conjunction with elevated levels of cortisol.
- Consistent with Task 4 and Task 5 we have conducted a refined analysis of multi-stability properties of both the broad HPA-HPG-immune model and the detailed BIS immune model. Comparing predicted equilibrium states with experimental immune and endocrine data from male and female GWI and CFS subjects we find:
    - Male GWI and CFS subjects align with states showing hypercortisolism, low testosterone, elevated Th1 inflammatory cytokines, decreased NK cell activity in conjunction with an

elevated Th17 response, although male CFS subjects also show a propensity to align with an elevated Treg response suggesting a mixed immune signature for this illness not seen in GWI.

  - Female CFS subjects align with states showing hypocortisolism, elevated estrogen, and a shift towards Th2 activation.

- We have re-assessed our approach to treatment design (Task 6, 7) and have begun encoding an approach based on a global search for a treatment course assisting an optimal walk through a discrete endocrine immune state space leading from an illness to a healthy condition.

Reportable Outcomes.
The results of these latest analyses are being communicated as follows:

- The previous draft manuscript Craddock et al., 2013, enclosed as Appendix A, has been extensively revised and is now submitted to the journal PLoS One. Similarly we expect the extensions and revisions to the detailed immune model (working document in Appendix B, Annual Report 2012, Fritsch et al., 2013), to be ready for submission to the journal Molecular Systems Biology by October this year.
- Early results were presented at a closed meeting sponsored by the CDC and the CFIDS Association of America and held at the Cold Spring Harbor Laboratory's Banbury Centre in Long Island, NY (Sep. 30 -Oct 3, 2012).
- We will be submitting two abstracts for oral presentation at the IACFS/ME 11th Biennial International Research and Clinical Conference to be held in San Francisco, California, USA, March 20-23, 2014. The conference is co-sponsored by Stanford University.

Regarding synergy with complementary research efforts, these findings were recently used to secure an invited GWIRP Consortium Award, now awarded (prime institution - Nova Southeastern University). The are also being used in support of 2 VA Merit applications that have been reviewed and invited for resubmission this month.

Conclusions.
We are currently processing a formal request for a one-year no-cost extension of the project term due to a delayed start. We have carried out a major shift in paradigm and continue to refine these regulatory circuit models as well as developing new components such as the neuroinflammatory model. The basic algorithmic framework has now been translated and re-engineered to deploy larger more detailed models on distributed high-performance platforms like the Pegasus 2 platform at the University of Miami.

Simulations based on these models have shown that the illness-specific effects of gender are particularly striking. Work continues on the refinement of the intervention design component. Initial analyses favor the deployment of a joint hormone-immune intervention over strategies that target these systems separately.

Personnel receiving support from this award:

- Travis Craddock, Ph.D., Senior Research Associate, Broderick Clinical Systems Biology Laboratory, University of Alberta;
  *Now co-investigator and Assistant Professor of Psychology, Nova Southeastern University, F*L.
- Lundy McKibbin, undergraduate student MD class of 2017, Undergraduate Research Intern, Broderick Clinical Systems Biology Laboratory, University of Alberta;
- Simar Singh, M.Sc. graduate 2012, Graduate Research Intern, Broderick Clinical Systems Biology Laboratory, Nova Southeastern University, Institute for Neuro-immune Medicine
- Mark Rice, undergraduate student computer science, Research Intern and Chief Programmer, Nova Southeastern University, Institute for Neuro-immune Medicine; Clinical Systems Biology Group (Broderick and Craddock)

- Ryan del Rosario, undergraduate student MD class of 2017, Research Intern and Lead HPC Programmer, Nova Southeastern University, Institute for Neuro-immune Medicine; Clinical Systems Biology Group (Broderick and Craddock).

References.

1. Thomas R, Thieffry D, Kaufman M (1995) Dynamical behaviour of biological regulatory networks--I. Biological role of feedback loops and practical use of the concept of the loop-characteristic state. Bull Math Biol. 57: 247-276.
2. Thomas R (1991) Regulatory Networks Seen as Asynchronous Automata: A Logical Description. J Theor Biol 153: 1-23.
3. Mendoza L, Xenarios I (2006) A method for the generation of standardized qualitative dynamical systems of regulatory networks Theor Biol Med Model 3: 13.
4. Ben-Zvi A, Vernon SD, Broderick G. (2008). Model-based Therapeutic Correction of Hypothalamic Pituitary Adrenal Axis Dysfunction. PLoS Comput Biol 5(1): e1000273. doi:10.1371/journal.pcbi.1000273.
5. Brown M (1975). A method for combining non-independent, one-sided tests of significance. Biometrics 31: 987–992.
6. Craddock TJA, Miller DB, Fletcher MA, Klimas NG, Broderick G. (2013). Towards an Integrative Model of Complex Stress-Mediated Illnesses: Gulf War Illness and Chronic Fatigue Syndrome. *PLoS One, Submitted.*
7. Broderick G, Kreitz A, Fuite J, Fletcher MA, Vernon SD, Klimas N (2011). A pilot study of immune network remodeling under challenge in Gulf War Illness. Brain Behav Immun. Feb; 25(2): 302-13.
8. Broderick G, Fuite J, Kreitz A, Vernon SD, Klimas N, Fletcher MA (2010). Formal Analysis of Cytokine Networks in Chronic Fatigue Syndrome. Brain Behav Immun, Oct; 24(7): 1209-17.
9. Fuite J,Vernon SD, Broderick G (2008). Neuroendocrine and Immune Network Re-modeling in Chronic Fatigue Syndrome: An Exploratory Analysis. Invited submission, Genomics; 92(6): 393-399.
10. Folcik VA, An GC, Orosz CG (2007). The Basic Immune Simulator: an agent-based model to study the interactions between innate and adaptive immunity. Theor Biol Med Model. Sep 27;4:39.
11. Folcik VA, Broderick G, Mohan S, Block B, Ekbote C, Doolittle J, Khoury M, Davis L, Marsh CB (2011). Using an agent-based model to analyze the dynamic communication network of the immune response. Theor Biol Med Model. Jan 19;8:1.
12. Fritsch P, Craddock TJA, Smylie AL, Folcik Nivar VA, Fletcher MA, Klimas NG, de Vries G, Broderick G (2012). A Study of Multiple Homeostatic Regimes in a Discrete Logic Model of Immune Signaling. In preparation.
13. Broderick G, Ben-Hamo R, Vashishtha S, Efroni S, Nathanson L, Barnes Z, Fletcher MA, Klimas N. (2013). Altered immune pathway activity under exercise challenge in Gulf War Illness: an exploratory analysis. Brain Behav Immun. Feb;28:159-69.
14. Fletcher MA, Rosenthal M, Antoni M, Ironson G, Zeng XR, Barnes Z, Harvey JM, Hurwitz B, Levis S, Broderick G, Klimas NG.(2010). Plasma neuropeptide Y: a biomarker for symptom severity in chronic fatigue syndrome. Behav Brain Funct. Dec 29;6:76.

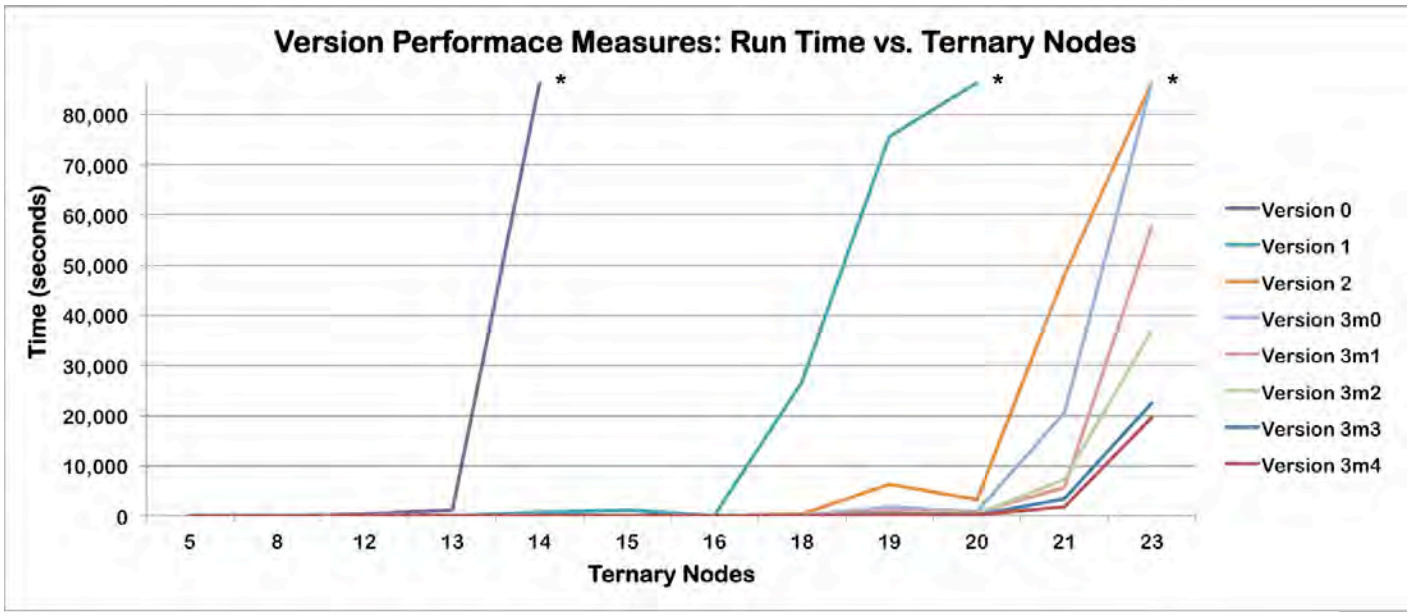

Figure 1. *Evolution of computational performance*. Evolution of computer wall time as a function model complexity described in terms of the number of state variables (ternary nodes). In less than a year, re-engineering of the computer code supporting the identification of stable states in a regulatory system has enable an almost 2-fold increase in the number of state variables in the circuit model.

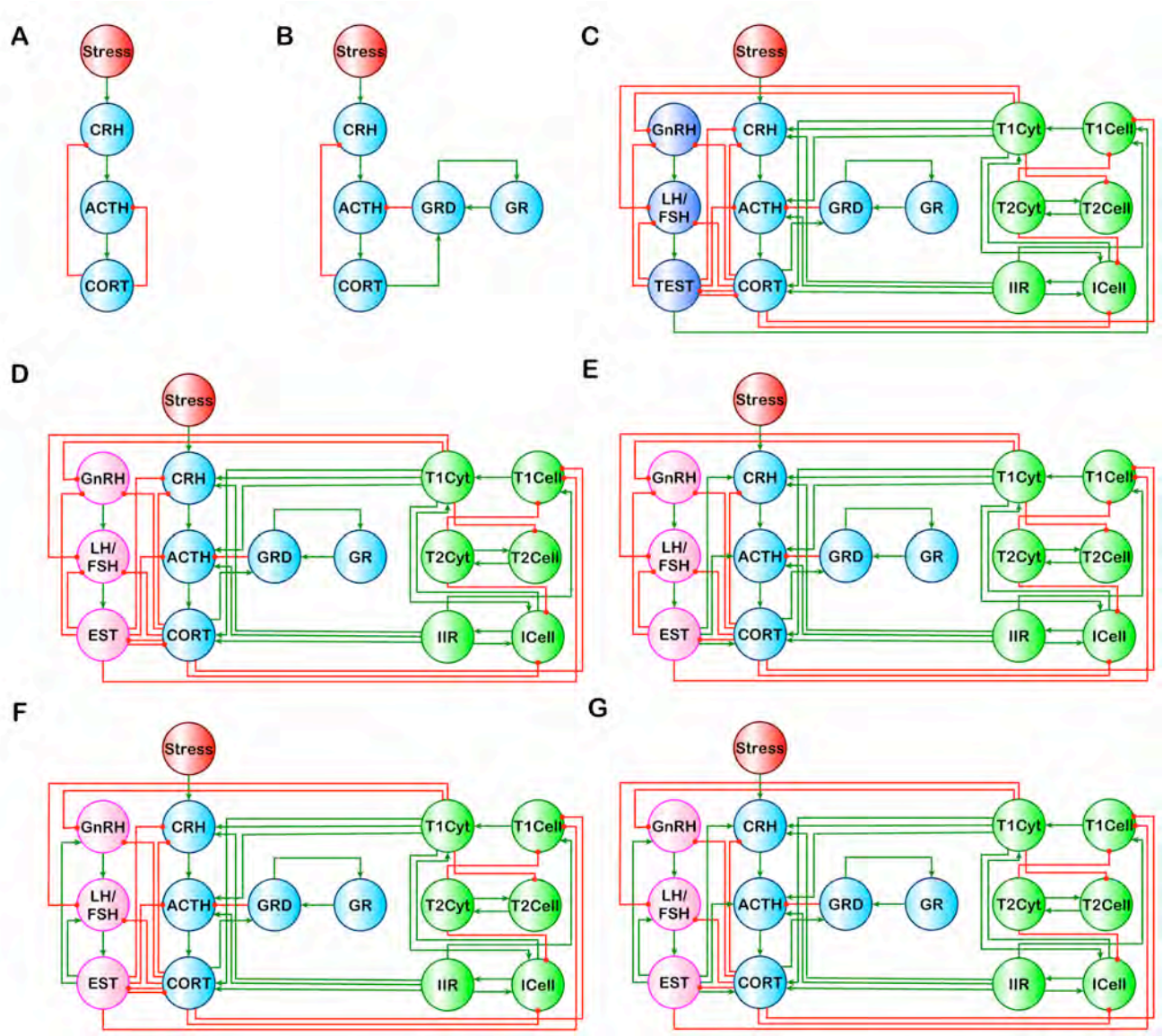

Figure 2. *Increased granularity multi-axis model*. A significant revision of the discrete circuit model of HPA function (A,B) augmented with HPG-immune interactions in male subjects (C) and female subjects (D-G) in the specific case of positive feedback along the female HPG axis and suppressive interaction with the HPA axis (revised and resubmitted manuscript) [6]. Green directed edges represent an up-regulation of the target by the source node whereas a red terminal edge represents a suppressive action.

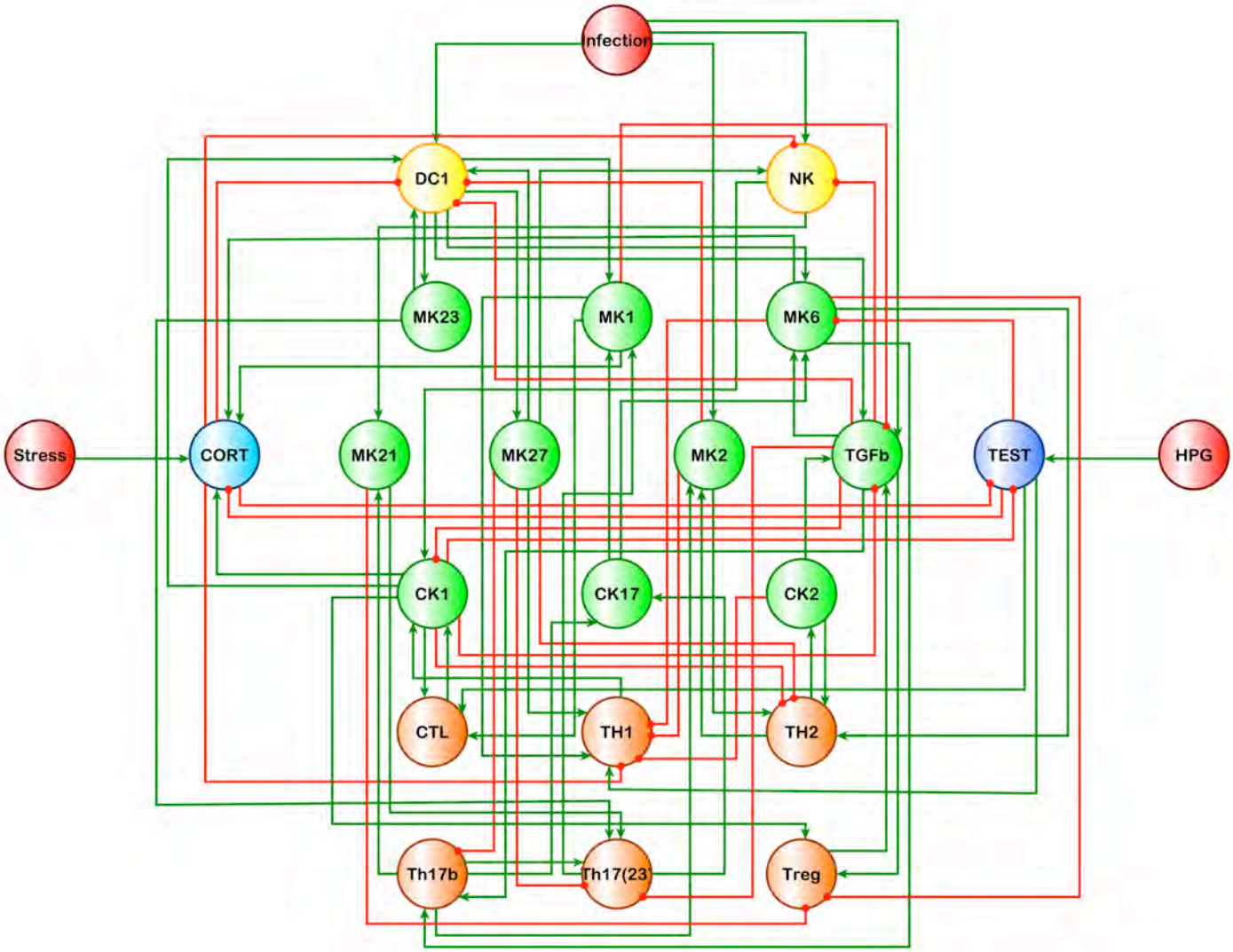

Figure 3. *Detailed Immune model revised*. Circuit diagram of the detailed immune system model revised to include elements of Th17 and Treg activity mediated by TGF-β, IL-21, IL-23, IL-27 and others. This is a significant increase in granularity from the previous such model and has resulted in a revision of draft manuscript, now underway and due for submission before year end [12].

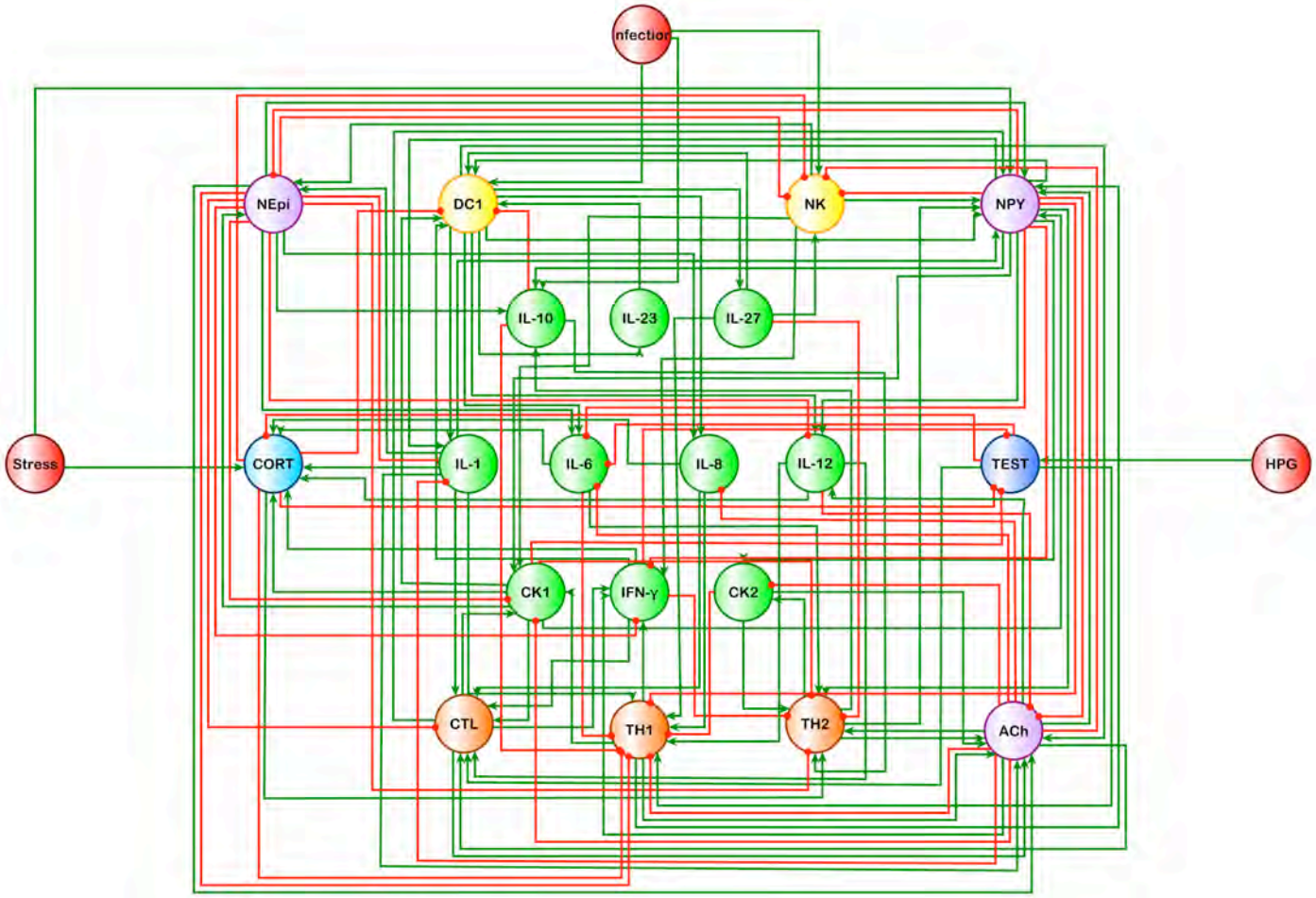

Figure 4. *High-resolution immune model with neurotransmission oversight*. Circuit diagram of a first prototype model capturing fine-grained immune signaling with the contribution of immune modulating neurotransmitters neuro-peptide Y (NPY), acetylcholine (ACh) and norepinephrine (NEpi). This model is still in progress and will incorporate the Th17 and Treg axes as well as additional neurotransmitters as we move forward.

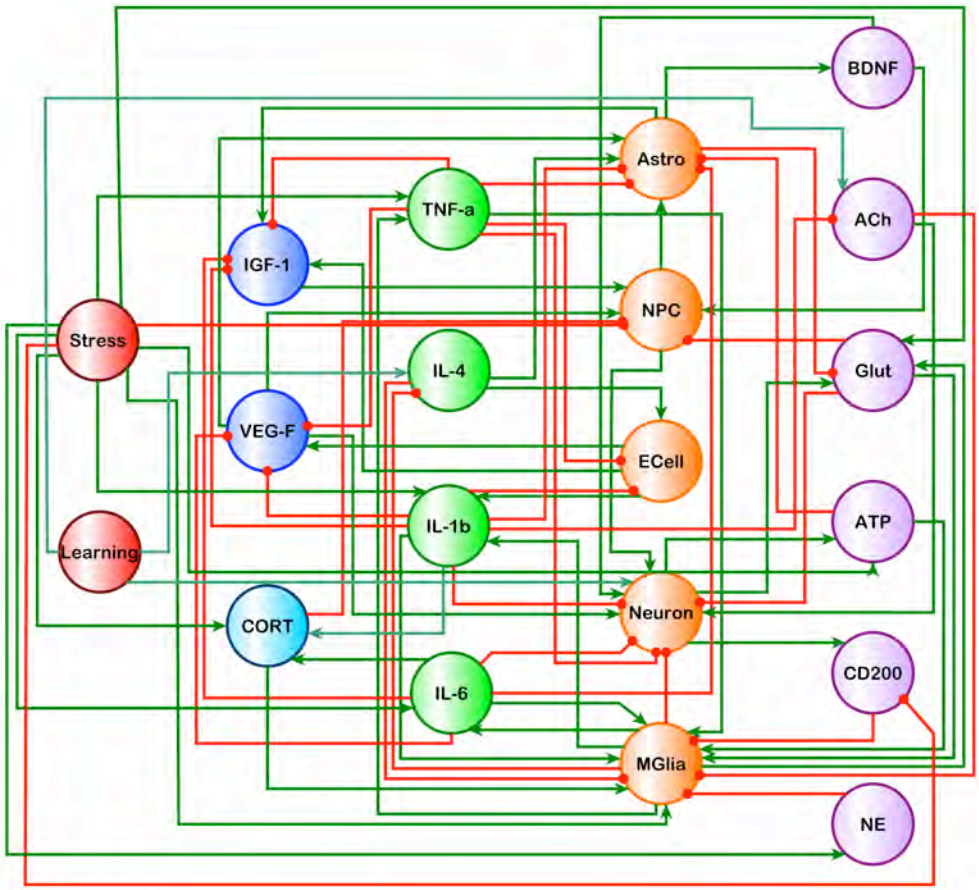

Figure 5. *A first prototype model of brain immunity*. A first circuit model describing the regulation of neuro-inflammation in the brain that includes the role of neurons, neural progenitor cells (NPCs), endothelial cells (ECells), microglia, and astrocytes as key cellular components as well as basic signaling mechanisms involving interleukin (IL)-1, IL-4, IL-6, tumor necrosis factor (TNF)-α, and OX-2 membrane glycoprotein (CD200) and other molecular messengers.

Appendix A:

Craddock TJA, Fritsch P, Rice MA Jr, del Rosario RM, Miller DB, Fletcher MA, Klimas NG, Broderick G. A Role for Homeostatic Drive in the Perpetuation of Complex Chronic Illness: Gulf War Illness and Chronic Fatigue Syndrome. 2013, *Submitted PLoS One, Under editorial review*.

A Role for Homeostatic Drive in the Perpetuation of Complex Chronic Illness: Gulf War Illness and Chronic Fatigue Syndrome

Travis J. A. Craddock**[1,2,3], Paul Fritsch[4], Mark A. Rice Jr.[3], Ryan M. del Rosario[3], Diane B. Miller[5], Mary Ann Fletcher[6], Nancy G. Klimas[3,7] and Gordon Broderick[1,3,4,8]

[1]Center for Psychological Studies, Nova Southeastern University, Fort Lauderdale, Florida, USA

[2]Graduate School for Computer and Information Sciences, Nova Southeastern University, Fort Lauderdale, Florida, USA

[3]Institute for Neuro-Immune Medicine, Nova Southeastern University, Fort Lauderdale, Florida, USA

[4]Department of Medicine, Faculty of Dentistry and Medicine, University of Alberta, Edmonton, Alberta, Canada

[5]Centers for Disease Control and Prevention, National Institute for Occupational Safety and Health, Morgantown, West Virginia, USA

[6]Department of Medicine, Miller School of Medicine, University of Miami, Miami, Florida, USA

[7]College of Osteopathic Medicine, Nova Southeastern University, Fort Lauderdale, Florida, USA

[7]College of Pharmacy, Nova Southeastern University, Fort Lauderdale, Florida, USA

** Corresponding author

Dr. Travis Craddock, Assistant Professor, Institute for Neuro-Immune Medicine, Nova Southeastern University, 3424 University Drive, Suite 3440, Fort Lauderdale, Florida, USA 33328

Ph: +1-954-262-2868 Email: tcraddock@nova.edu

Abstract

A key component in the body's stress response, the hypothalamic-pituitary-adrenal (HPA) axis orchestrates changes across a broad range of major biological systems. Its dysfunction has been associated with numerous chronic diseases including Gulf War Illness (GWI) and chronic fatigue syndrome (CFS). Though tightly coupled with other components of endocrine and immune function, few models of HPA function account for these interactions. Here we extend conventional models of HPA function by including feed-forward and feedback interaction with sex hormone regulation and immune response. We use this multi-axis model to explore the role of homeostatic regulation in perpetuating chronic conditions, specifically GWI and CFS. An important obstacle in building these models remains the scarcity of *in vivo* kinetic data. We circumvented this using a discrete logic representation based solely on literature of physiological and biochemical connectivity to provide a qualitative description of system behavior. This connectivity model linked molecular variables across the HPA axis, hypothalamic-pituitary-gonadal (HPG) axis in men and women, as well as a simple immune network. Inclusion of these interactions produced at multiple alternate homeostatic states. Experimental data for endocrine-immune markers measured in male GWI subjects showed the greatest alignment with predictions of a naturally occurring alternate steady state presenting with hypercortisolism, low testosterone and a shift towards a Th1 immune response. In female CFS subjects, expression of these markers aligned with an alternate homeostatic state displaying hypocortisolism, high estradiol, and a shift towards an anti-inflammatory Th2 activation. These results support a role for homeostatic drive in perpetuating dysfunctional cortisol levels through persistent interaction with the immune system and HPG axis. This same basic drive may also perpetuate sexually dimorphic responses due to inherently different behavior of the male and female HPG. Though coarse, these models may nonetheless support the design of robust treatments that might exploit these regulatory regimes.

53 **Introduction**

54 The hypothalamic-pituitary-adrenal (HPA) axis, a key component in the body's stress
55 response, serves to articulate changes in a broad range of homeostatic regulators as a
56 function of environmental cues. Such cues can consist of both physical stressors (injury,
57 infection, thermal exposure) and psycho-emotional stressors (frustration, fear, fight or flight
58 decisions). Instantiation of this survival program is accomplished through controlled
59 modulation of the neuroendocrine and immune systems, as well as the sympathetic nervous
60 systems [1-3]. Considering its function as a broad-reaching integrator of major physiological
61 systems, it is no surprise that numerous chronic conditions have been associated with
62 abnormal regulation of the HPA axis, including major depressive disorder (MDD) [4, 5], post-
63 traumatic stress disorder (PTSD) [6-8], Alzheimer's disease [9], Gulf War Illness (GWI) [10-
64 12], and chronic fatigue syndrome (CFS) [13-15]. When compared to non-deployed
65 veterans, Golier et al. [10] found that symptomatic Gulf War veterans without psychiatric
66 illness, as well as veterans with PTSD alone, showed significantly greater cortisol
67 suppression to dexamethasone (DEX) suggesting markedly enhanced negative feedback
68 along the HPA axis. Further study by these same investigators indicated that this might be
69 due to a significantly attenuated ACTH response by the pituitary in veterans with GWI
70 without PTSD [11, 12]. A similar suppression of cortisol response to DEX was found in CFS
71 subjects by Van Den Eede et al. [13] with this being further exacerbated by oestrogen
72 intake. With regard to HPA circadian dynamics, CFS subjects were found to exhibit
73 significantly increased adrenal sensitivity to ACTH and marginally increased inhibitory
74 feedback during the nocturnal period when compared with control subjects and CFS
75 subjects comorbid with fibromyalgia (FM) [14, 15]. Conversely the pain-dominant CFS-FM
76 subjects showed significantly blunted cortisol inhibitory feedback. While evidence such as
77 this implicates abnormal regulation of HPA function leading to chronic hypocortisolic and
78 hypercortisolic states in these illnesses, the genesis of this dysregulation is unclear.
79

Previously we investigated the possibility that some of these pathological states may coincide with naturally occurring alternate homeostatic stable states [16]. These “backup programs” would offer a way of maintaining homeostatic control in crisis situations at the cost of reduced function. The existence of such multiple stable states is characteristic of systems that incorporate feed-forward and feedback mechanisms. Feedforward loops in biology play the crucial role of driving rapid acute responses, while feedback loops will generally limit the extent of a response. Both will also drive complex dynamic behavior, including differentiation and periodicity [17]. While small perturbations may force temporary departures, these systems return to their original resting states once these perturbations are removed. If however, the perturbation is of significant strength and duration, the system may be incapable of returning to its normal operating regime and instead may assume a new alternate resting state. Knowledge of the system dynamics can allow us to map these different stable states and several mathematical models of the HPA exist [18-26]. So far, only one such model is known to accommodate multi-stability in the dynamic behavior of the HPA axis. It does so via the addition of a feed-forward mechanism involving dimerization of the glucocorticoid receptor (GR) complex [27] (Figure 1). In this process glucocorticoid (GC) bound GRs form homodimers that translocate into the cell nucleus to bind DNA, up-regulating GR synthesis and producing a positive feedback loop. However, this model and the majority of other models do not extend beyond the physiological boundaries of the HPA axis itself and thus are limited in their predictive capabilities. As discussed in the following sections, HPA activity is intertwined with the behavior of the hypothalamic-pituitary-gonadal (HPG) axis and the immune system, among others, and this interplay should not be ignored when considering the number and nature of stationary states available to the overarching system. Our hypothesis is that these alternate regulatory regimes may facilitate the persistence of complex chronic illnesses like GWI and CFS. To evaluate the role of alternate homeostatic attractors in these illnesses we constructed a computational model of regulatory control linking the HPA, HPG and immune systems.

There is a substantial body of physiological and biochemical data for many biological systems describing the connectivity between molecular and cellular elements, the presence of recurring structural motifs and functional modules. For example, negative autoregulation, in which a transcription factor represses its own transcription, is a simple network motif observed in many transcription networks. While, numerous motifs have been found in biological networks (negative/positive autoregulation, coherent/incoherent and multi-output feedforward loops, single-input modules and dense overlapping regulons) [28], data regarding the precise stoichiometry and kinetics of these systems in humans is extremely limited. Many existing models rely heavily on animal data as a source of kinetic parameters, or adopt general order of magnitude estimates when this data is lacking. To circumvent this issue and draw on the rich body of known molelcular and cellular interactions in physiological and biochemistry, we have adopted the discrete logical network methodology proposed originally by Thomas et al. [29, 30] and developed further by Mendoza and Xenarios [31]. By applying logic rules to a network of known interactions it is possible to identify the number of stable resting states, their type as well as their molecular and cellular description, without detailed knowledge of the response dynamics. In this work we use this method to extend our previous analysis of human HPA axis dynamics by including its regulatory interactions with the neighboring HPG axis and immune system. This resulting mathematical model better represents the complexity of endocrine-immune interactions by supporting the detection and identification of alternate resting modes of the HPA-HPG-immune axis. Based on connectivity information alone, we show that multi-stability is easily obtained from these interacting systems. Moreover, we show that experimental data from our on-going studies of GWI and CFS show better alignment with these alternate resting modes than with the typical healthy homeostatic stable state. Ultimately, knowledge of such homeostatic modes could be used to identify promising applications of pharmaceutical, hormone and/or immune therapy that exploit the body's natural dynamics to reinforce treatment effects.

136 **Methods**

137 **Ethics Statement**

138 All subjects signed an informed consent approved by the Institutional Review Board of the
139 University of Miami. Ethics review and approval for data analysis was also obtained by the
140 IRB of the University of Alberta.

141

142 **An Integrative Multi-systems Model of the HPA-HPG-Immune System**

143 There is a substantial amount of physiological data describing the HPA, HPG and immune
144 systems as stand-alone entities. To a much lesser degree there also exists evidence for the
145 mutual interactions between these systems. The following sections describe the
146 experimental evidence used to infer the topology of an overarching HPA-HPG-immune
147 interaction network (Figure 1).

148

149 **The HPA Axis:** Activation of the HPA axis begins at the paraventricular nucleus (PVN) of
150 the hypothalamus. Specifically, afferents transmitting stress related information in the brain
151 converge on the medial parvocellular neurons of the PVN inducing the release of several
152 peptides, including corticotropin-releasing hormone (CRH) and arginine vasopression (AVP),
153 into the pituitary hypophysial-portal circulation. The unique vascular system allows very
154 small quantities of these hypothalamic hormones to act directly on their targets in the
155 anterior pituitary without dilution by systemic circulation. CRH and AVP act in conjunction on
156 membrane bound CRH-R1 receptors in the anterior pituitary to stimulate adrenocorticotropic
157 hormone (ACTH) synthesis, and its rapid release into peripheral circulation. ACTH
158 circulates to the adrenal cortex where it acts on the membrane bound MC2-R receptor to
159 simulate the release of GCs (corticosterone in the rat, and cortisol (CORT) in humans and
160 nonhuman primates). To regulate the stress response, GCs exert negative feedback at the
161 hypothalamus and pituitary to inhibit further synthesis and release of CRH and ACTH,
162 respectively [32]. This is the standard view of the HPA axis utilized in the majority of models
163 (Figure 1 A). However, as noted by Gupta et al. [27] circulating glucocorticoids act via

164 cytostolic GRs, which, unlike membrane bound receptors, dimerize (GRD) and translocate
165 into the cell nucleus upon activation to up-regulate GR synthesis and interact with other
166 relevant transcription factors, or GC-sensitive genes (Figure 1 B). Gupta et al. included this
167 GR expression feedforward loop at the pituitary, as it is a main driver of the HPA axis, and
168 found a resulting bistability in the HPA system [27]. However, all nucleated cells possess
169 GRs, as GCs influence practically every system in the body, suggesting this feedforward
170 loop may be important in other tissues beyond the HPA axis. As described below major
171 systems affected by GCs include the HPG axis and immune system.
172
173 **The HPG Axis:** GCs have an inhibitory effect on the HPG axis, a central regulator of the
174 reproductive system, at all levels [33-37]. Activation of the HPG starts from brain generated
175 pulsatile signals that stimulate the preoptic area of the hypothalamus to produce
176 gonadotropin-releasing hormone (GnRH). GnRH is secreted into the pituitary hypophysial
177 portal bloodstream, which carries it to the pituitary gland, where it activates membrane
178 bound GnRH-R receptors, resulting in the synthesis and secretion of luteinizing homone
179 (LH) and follicle-stimulating hormone (FSH) into circulation. These gonadotropins flow to the
180 gonads where they work synergistically to promote the secretion of the sex steroids. In
181 males, LH binds to receptors on Leydig cells in the testes to stimulate the synthesis and
182 secretion of testosterone (TEST). In females, LH activates receptors on Theca interna cells
183 in the ovaries to stimulate the release of androstenedione, which is aromatized by granulosa
184 cells to produce estradiol (EST), and progesterone (PROG). TEST negatively feeds back on
185 the HPG to inhibit GnRH, FSH and LH secretion and synthesis [33]. This feedback
186 mechanism is somewhat more complex in females where, depending on the phase of the
187 female menstrual cycle, EST and PROG can exert either positive or negative feedback on
188 the production and release of GnRH and the gonadotropins [36, 38, 39].
189
190 A lesser-known aspect is that several components of the HPG axis exert reciprocal effects
191 on the HPA axis [33, 34, 36]. Testosterone exhibits an inhibitory effect on all levels of the

192 HPA [33] (Figure 1 C), whereas EST and PROG can serve to stimulate or inhibit the HPA
193 axis depending on menstrual cycle phase, or phase of life [34]. These affects may be
194 mediated through changes in adrenocorticoid synthesis, stress-induced ACTH and GC
195 release, and CRH and AVP synthesis in the PVN, by direct activation of oestrogen and
196 androgen receptors along the HPA or via interaction between GRs and sex steroid receptors
197 to regulate transcription [33,34,36]. Thus, an interactive functional crosstalk exists between
198 the HPA and HPG axes, which cannot be ignored when investigating HPA axis regulation
199 and dysfunction. Mutual inhibition between the HPA and HPG (Figure 1 C) was considered
200 standard for males. However, as it is not clear whether the EST and PROG
201 inhibition/stimulation of the HPA occurs in coordination with the inhibition/stimulation of the
202 HPG, these cases were explored for females alone as separate alternative models of the
203 HPA-HPG interaction (Figure 1 D-G) in addition to the model considered for males.
204
205 **A Simple Model of the Immune System:** While not typically considered part of the
206 neuroendocrine system, the immune system plays a very important role in regulating the
207 HPA axis. Here we base our simplified immune system upon our previous work detailing the
208 communication network of the immune response [40]. Cells of the innate immune response
209 (ICells), including mononuclear phagocytes, such as macrophages, and dendritic cells,
210 natural-killer (NK) cells, endothelial cells and mucosal epithelial cells, communicate via the
211 release of numerous cytokines. Cytokines that regulate the innate immune response (IIR)
212 include interleukin (IL) -1, IL-6, IL-8 and tumor necrosis factor alpha (TNF-α), and can also
213 include IL-12, a primary mediator of early innate immunity. Primarily, these signals serve to
214 activate and recruit other ICells, which in turn produce more cytokines. IL-15, which
215 stimulates proliferation of NK cells and effector T-lymphocytes, can also be considered as
216 part of the IIR as well as IL-23, an important inflammatory signal contributing to the Th17
217 response against infection.
218

219 IIR signals can also serve to prime helper T cells towards a Th1 type adaptive immune
220 response (T1Cell). This response produces Th1 proinflammatory cytokines (T1Cyt)
221 including IL-2, interferon-gamma (IFN-γ), and tumor necrosis factor beta (TNF-β), which
222 further activates ICells, while suppressing the Th2 adaptive immune response (T2Cell).
223 The T2Cell is responsible for the production of the Th2 anti-inflammatory cytokines (T2Cyt)
224 IL-4, IL-5, IL-10 and IL-13, which have important anti-inflammatory and immunosuppressive
225 activities, and serve to inhibit the activity of T1Cell and ICells.
226
227 Cytokines can also serve as mediators between the immune and endocrine systems.
228 Between the HPA and the immune network there exists a mutual crosstalk [41-43] (Figure 1
229 C-G). The IIR and T1Cell cytokines selected here serve to stimulate the HPA axis at all
230 levels [41-43]. CORT, in turn, acts to suppress the activity of ICells (specifically NK cells
231 [44], and DC cells [45]), and the T1Cell [46] causing a shift from the inflammatory to the anti-
232 inflammatory response [41, 42, 47]. The interaction between the HPG and the immune
233 system is complex and sexually dimorphic, and is still an active field of research. However,
234 at a general coarse level of description TEST serves to stimulate the development of the
235 Th1 response [48] (Figure 1 C), whereas EST inhibits the Th1 response causing a shift
236 towards the Th2 anti-inflammtory response [48,49]. The reciprocal crosstalk from the
237 immune system to the HPG is equally intricate. In broad terms this conversation is
238 communicated via T1Cyt. Receptors for TNF-α and IFN-γ are expressed in testicular Leydig
239 cells and there is evidence that these cytokines can directly inhibit testosterone production
240 [50]. TNFα also decreases the release of GnRH in the hypothalamus and LH in the pituitary
241 gland in both males [50] and females [51] eventually leading to a decrease in sex steroid
242 levels. As such, we model the T1Cyt as inhibiting GnRH and LH/FSH in both male and
243 female models.
244
245
246

A Discrete State Representation

Following the methods of Thomas et al. [29, 30], and more recently Mendoza and Xenarios [31], the neuroendocrine-immune system was represented as a connectivity model consisting of interconnected molecular and cellular variables with three discrete states: -1 (inhibited), 0 (nominal) and 1 (activated). According to this type of model the current state of all variables in a system is described by a state vector $\vec{x}(t)$, such that:

$$xt=x1t,x2t,...,xNt \quad (1)$$

where $x_N(t)$ is the state of the Nth variable of the system at time *t*. The image vector $\vec{x}(t+1)$ describes the preferred state towards which the system evolves in the next time increment. The state value of the image vector for the ith variable is determined from its current state and a set of balanced ternary logic statements based on the current value of variable and the mode of action (i.e. activate or inhibit) of the neighboring input variables. These logic statements are expressed as follows (Eq. 2):

$$xit+1=(xi1At\vee xi2At...xijAt)\nabla(xi1It\vee xi2It...xikIt)(xi1At\vee xi2At...xijAt)\neg(xi1It\vee xi2It...xikIt) \quad (2)$$

where the ∇, $\vee$, and $\neg$ symbols are ternary HIGH/LOW PASS, OR and NOT operators, x_{ij}^{A} is the state of the ith variable's j^{th} activator, x_{ik}^{I} is the state of the ith variable's k^{th} inhibitor. The ternary operators given in Equation (2) are described in further detail in Supplementary Tables 1- 3. The first entry in Equation (2) is used when the variable possesses both activators and inhibitors, the middle when the variable has only activators and last when the activator has only inhibitors.

Applying Equation (2) to each variable in the model for the mth state of the system, $\vec{x}^{m}(t)$, defines the image vector $\vec{x}^{m}(t+1)$ for that state. With $\vec{x}^{m}(t+1)$ defined, the system may be updated asynchronously (allowing only one variable to change at a time) following the

generalized logical analysis of Thomas et al. [29, 30]. According to this method the ith variable of the mth state vector $\vec{x}^m(t)$ is moved one step towards its preferred image $\vec{x}^m(t+1)$ (e.g. If $\vec{x}^m(t)$ = -1 and $\vec{x}^m(t+1)$ = 1, then $\vec{x}_i(t)$ is set to 0). Thus, for each current state of the system there are potentially several subsequent states towards which it may asynchronously evolve.

The number of states, and the values they can be assigned, determine the total number of states available to the model system. With the ternary logic used here, a model of N variables possesses 3^N states. As a result, the number of states increases rapidly as new variables are added. By analyzing all possible states of the system a temporal sequence of states may be discerned. To interpret the results, each state of the system can be represented as an element in a graph. The evolution from one state to a subsequent state can be represented as a directed edge between the two states in this graph. Representation of the state trajectories in this fashion makes it possible to draw on the concepts and tools of graph theory for analysis of the system dynamics. Steady states are defined as those states for which the image vector is the same as the current state vector; in other words the state possesses an out degree of 0.

Comparison to Model

GWI Cohort Sample Collection: Similar cytokine profiles and endocrine measures were obtained as part of a larger ongoing study of 27 GWI and 29 HC subjects recruited from the Miami Veterans Administration Medical Center. Subjects were male with an average age of 43 years and BMI of 28. Inclusion criteria was derived from Fukuda et al. [52], and consisted in identifying veterans deployed to the theater of operations between August 8, 1990 and July 31, 1991, with one or more symptoms present after 6 months from at least 2 of the following: fatigue; mood and cognitive complaints; and musculoskeletal complaints. Subjects

300 were in good health prior to 1990, and had no current exclusionary diagnoses [53]. Use of
301 the Fukuda definition in GWI is supported by Collins et al. [54]. Control subjects consisted of
302 gulf war era sedentary veterans and were matched to GWI subjects by age, body mass
303 index (BMI) and ethnicity. Additional details regarding this cohort and the laboratory assays
304 performed are available in Broderick et al. [55].
305
306 **CFS Cohort Sample Collection:** Levels of cortisol (CORT) and estradiol (EST) measured
307 in peripheral blood were obtained from the Wichita Clinical dataset [56] for a group of 39
308 female CFS subjects and 37 Healthy controls (HCs) with an average age of 52 years and an
309 average body mass index (BMI) of 29. Additional details of this cohort and the laboratory
310 assays performed may be found in work previously reported by our group [57, 58]. Multiplex
311 cytokine profiles were obtained in plasma from a separate but demographically comparable
312 cohort of 40 female CFS subjects and a group of 59 healthy female matched control
313 subjects studied by our group at the University of Miami [59]. Average age in this cohort was
314 53 years with an average BMI of 26. Profiling of cytokine concentrations was performed in
315 morning blood plasma samples using an enzyme-linked immuno-absorbent assay (ELISA)-
316 based assay. Details of this protocol and results of a comparative analysis of cytokine
317 expression patterns are available in Broderick et al. [59]. In both studies a diagnosis of CFS
318 was made using the International Case Definition [53,60]. Exclusion criteria for CFS included
319 all of those listed in the current Centers for Disease Control (CDC) CFS case definition, as
320 well as psychiatric exclusions, as clarified in the International CFS Working Group [60].
321
322 **Statistical Analysis:** Brown's theoretical approximation [61] of Fisher's statistics was used
323 to calculate the significance of alignment between experimental data and a given model
324 predicted state . Fisher's method, a meta-analysis technique, combines probabilities to
325 obtain the overall significance of a set of *P*-values obtained from independent tests of the
326 same null hypothesis. The combined χ^2 statistic,

$$T0=-2i=1N\ln(pi) \quad (3)$$

where N is the number of measureable variables and p_i is the corresponding P-values under the null hypothesis, has a χ^2 distribution with $2N$ degrees of freedom assuming that the performed tests are independent. As the molecular variables of the endocrine and immune system interact with one another, as evidenced by the above connectivity diagrams, they are not independent. As a result, direct application of this test statistic is invalid, since the assumption of independence is violated. Brown [61] suggested a method for combining non-independent tests. If the tests are not independent, then the statistic T_0 has mean m = $2N$ and variance (σ^2) given as,

$$\sigma 2=4N+2i=1N-1j=i+1Ncov(-2\ln pi,-2\ln pj) \quad (4)$$

where p_i and p_j are the P-values for each test and the covariance (cov) is calculated as,

$$cov(-2\ln pi,-2\ln pj)=\rho ij(3.25+0.75\rho ij), \quad \& \quad 0\leq\rho ij\leq 1\rho ij(3.27+0.71\rho ij), \ -0.5\leq\rho ij\leq 0 \quad (5)$$

with ρ_{ij} being the unadulterated correlation between variable i and variable j. Finally, the overall significance P of a set of non-independent tests is calculated using the statistic T which under the null hypothesis follows the central χ^2 distribution, where $T = T_0/c$ with 2N/c degrees of freedom and $c = \sigma^2/4N$.

Here, we test if each experimental measure aligns with a given model predicted state. Our null hypothesis is that the experimental measures do not align. P-values for individual variables, p_i, are calculated using two-sample t-tests between ill subjects and healthy controls. Where model predictions give a variable as high (+1), 'right-handed' one-tailed test are used, whereas a 'left-handed' test was used when model predictions are low (-1), to give the probability of obtaining the predicted value when the null hypothesis is true. For the case where the model predicts normal behavior for a variable (0) a two-tailed t-test is used. However, the p-value from the two-tailed test, $p_{two\text{-}tail}$, gives the probability that there is an observable difference between illness and control, which is the null hypothesis. To rectify

354 this, when comparing to a model predicted variable of 0 we take the P-value to be $p_i = 1 -$
355 $p_{two\text{-}tail}$, giving the probability of obtaining the predicted value when the null hypothesis is true.
356
357 All cohort data was normalized using a Log2 transformation before T-tests and correlation
358 calculations were performed. The unadulterated correlation values ρ_{ij} between two
359 variables i and j were calculated in healthy subjects as the pairwise Pearson's linear
360 correlation coefficient between variables . The above-mentioned experimental data was
361 compared against model predictions based on the five measureable variables, namely
362 TEST/EST, CORT, IIR, T1Cyt, and T2Cyt. Where model variables represent an aggregate
363 set of markers each experimentally measured constituent marker was compared individually
364 to the model predicted value. For example, T1Cyt is composed of IL-2, IFNγ and TNFβ,
365 therefore 3 individual P-values were calculated based on the predicted value of T1Cyt.
366
367 **Results**
368 **Stable States in the HPA Models**
369 Application of the discrete state representation to the basic stand-alone HPA model (Figure
370 1 A) generated 27 system states, and failed to produce multiple stable states (Figure 2).
371 This is consistent with previous ordinary differential equation based models of this basic
372 representation of the HPA axis [21-26]. Discrete state representation of the HPA-GR model
373 (Figure 1 B) generated 243 system states. Of these, 2 system states possessed no
374 outbound edges and were stable attractor steady states (Figure 2). In the first steady state
375 all state variables assumed nominal values whereas the second steady state corresponded
376 to activation of state variables GRD and GR with suppression of ACTH and CORT. Once
377 again this solution is consistent with that obtained by analysis of the ordinary differential
378 equation model of the HPA-GR system proposed by Gupta et al. [27] and Ben Zvi et al. [16].
379
380 Combining the HPA-GR axis with the HPG axis and immune system (Figure 1 B-G)
381 altogether produced 4,782,969 system states. For the male HPG (model a) (Figure 1 C),

382 and three of the four female HPG models (models b, d and e) (Figure 1 D,E,G) five steady
383 states were identified (Figure 2). One stable state is characterized by nominal values for all
384 variables (SS0), which corresponds to the typically normal resting state of the system. The
385 first alternate state (SS1) displays low ACTH with high GRD and GR, while the second
386 (SS2) has inhibited innate and Th1 immune responses (low ICell, IIR, T1Cell, and T1Cyt),
387 with increased Th2 activity (high T2Cell and T2Cyt). The third stable state (SS3) appears to
388 be a combination of SS1 and SS2 with low ACTH, ICell, IIR, T1Cell and T1Cyt, and high
389 GRD, GR, T2Cell and T2Cyt. The final state (SS4) presents with hypercortisolism,
390 suppressed TEST and a shift towards the Th1 immune reponse (low T2Cell, T2Cyt, GnRH,
391 LH/FSH and TEST/EST, and high CORT, GRD, GR, T1Cyt and T1Cell). The persistently
392 low CORT state seen in the previous stand-alone HPA models of Gupta et al. [16] and Ben
393 Zvi et al. [27], was not recovered here. Instead, CORT was expressed at a nominal or high
394 value for all predicted states. SS1 most closely resembles the results of Gupta et al. [27],
395 and Ben Zvi et al. [16], however these previous models only considered a single regulator of
396 CORT, namely ACTH. The lack of a predicted hypocortisolic state in SS1 here can be
397 attributed to the interplay of multiple regulators of CORT (ACTH, IIR, TEST/EST, and
398 T1Cyt). Inclusion of additional regulators is not expected to further alter this state.
399
400 In the final female HPG model (model c) (Figure 1 F), corresponding to the ovulation phase,
401 these same five states were recovered along with six new additional states (Figure 2). In the
402 first three additional states the HPA axis and innate immune response are suppressed with
403 low CRH, ACTH, CORT, ICell and IIR, while the HPG and anti-inflammatory response are
404 raised with high T2Cell, T2Cyt, GnRH, LH/FSH and EST. The difference between the three
405 states is noted in the level of glucocorticoid receptor response, GR and GRD, which together
406 take values of low (SS5), nominal (SS6) and high (SS7). The remaining three additional
407 states all give suppressed HPA (CRH, ACTH, and CORT) and lowered T1Cell activity, with
408 high HPG activity (GnRH, LH/FSH and EST), and are again differentiated by their
409 glucocorticoid receptor levels (GR, GRD): low (SS8), nominal (SS9) and high (SS10).

410

411 Overall, inclusion of the simplified immune system and the HPG works to regulate CORT
412 levels in the HPA axis. The male HPG (HPG model a), and the majority of female HPG
413 configurations (HPG models b, d and e), serve to produce either nominal values of CORT,
414 with the potential of a shift towards Th2 activation (SS2 and SS3), or a hypercortisolic state
415 with low TEST/EST and a shift towards Th1 (SS4). Only connections associated with the
416 female gender (HPG model c) were responsible for the emergence of a natural
417 hypocortisolic state (SS5 – SS10). This hypocortisolic state comes with high EST and may
418 have a shift towards Th2 activation in the immune system.

419

420 **Comparison of GWI and CFS to Predicted States**

421 Application of Brown's meta-analysis method allowed for the calculation of a combined P-
422 value comparing the experimental data with the predicted stable states, allowing for the
423 alignment between different predicted stable states to be ranked. As experimental
424 measures allowed for comparison with only five variables (TEST/EST, CORT, IIR, T1Cyt,
425 and T2Cyt) several of the predicted stable states resulted in the same experimental profile
426 and resulting combined P-value despite being distinct states (e.g. SS0 and SS1 both show
427 nominal values for the five measureable variables).

428

429 To compare to our model the difference between steroid and cytokine levels recorded in
430 male Gulf War veterans with GWI and HCs were compared to the steady state values
431 predicted by the male variant of the HPA-GR-Immune-HPG model (model a). Comparison
432 to the nominal states (SS0/SS1) showed poor alignment, $P_{SS0/SS1} = 0.82$, suggesting that the
433 GWI profile cannot be considered the same as nominal behavior. Alignment with states
434 presenting a shift towards Th2 immune activation (SS2/SS3) showed better alignment,
435 $P_{SS2/SS3} = 0.38$, although with low significance. The final state, displaying hypercortisolism,
436 low TEST and a shift towards Th1 immune activation (SS4), yielded the best alignment, P_{SS4}
437 $= 0.30$, again however, with a low overall significance.

438

439 The difference between steroid and cytokine levels of female CFS subjects and HCs were
440 compared to the steady state values predicted by the female variants of the HPA-GR-
441 Immune-HPG models (model b-e). Again, alignment with states presenting nominal
442 changes in measureable variables (SS0/SS1) was poor, $P_{SS0/SS1} = 0.83$, supporting that CFS
443 is distinctly different from normal behavior. The Th2 shifted immune profile states
444 (SS2/SS3) showed a significant alignment, $P_{SS2/SS3} = 0.04$, suggesting Th2 activation in
445 CFS. This is further supported by low alignment with the Th1 immune activated state, with
446 hypercortisolism, and low EST (SS4), $P_{SS4} = 0.28$. Improved alignment is seen in states with
447 a shift towards Th2, coupled with hypocortisolism, and high EST (SS5/SS6/SS7), $P_{SS5/SS6/SS7}$
448 $= 0.02$, suggesting that these features contribute to the CFS profile. This is also supported
449 by low alignment with states only presenting hypocortisolism and high EST with no immune
450 activation (SS8/SS9/SS10), $P_{SS8/SS9/SS10} = 0.60$.

451

452 **Discussion**

453 The existence of multiple stable states is a prime characteristic of systems incorporating
454 feedforward and feedback mechanisms, and plays a critical part in guiding the complex
455 dynamics observed in biology. These alternate stable regulatory regimes occur due to the
456 feedforward and feedback mechanisms within the system and may allow escape routes for
457 survival of an insult and provide support in the medium or long-term to what is equivalent to
458 an uneasy cease-fire or adaptive compromise. An example of such compromises in
459 functional status in exchange for survival include vasovagal response to decreased blood
460 pressure and syncope ("fainting") [62]. From an evolutionary perspective it would be
461 advantageous for a pathogen to establish an adaptive relationship with the host. As naturally
462 occurring alternate states of homeostasis are inherently stable exploiting, these regimes
463 could be an advantageous way for a pathogen to establish long-term chronic infection, in
464 essence using the body's own homeostatic drive to maintain the status quo. To explore this
465 hypothesis, we constructed a simple but integrated model incorporating three of the body's

466 major regulatory axes: the HPA, the HPG and the immune system. Modeling the dynamic
467 properties of these complex systems presents a significant challenge, as much of the
468 detailed information describing in vivo kinetics in humans is unavailable. However, there is a
469 very significant body of connectivity data describing the interactions between the molecular
470 and cellular elements of these biological systems. To make use of this wealth of information
471 we have applied a discrete state representation to the neuroendocrine immune system
472 based solely on the biological connectivity found in the literature and a set of ternary logical
473 rules. Using a discrete logic methodology proposed by Thomas [30], we demonstrated that
474 the inclusion of feedforward/feedback loops leads to multiple stable states. Indeed, addition
475 of the positive feedback loop regulating glucocorticoid receptor dimerization (GR-GRD) to a
476 basic model of the HPA axis generated an alternate homeostatic state characterized by high
477 receptor expression and low circulating cortisol levels, a result found previously by Gupta et
478 al. [27] and Ben Zvi et al. [16] using differential equation based models. So dependent is the
479 natural emergence of these states on the regulatory wiring that inclusion of this receptor
480 dimerization in a more complex HPA-Immune-HPG models resulted in the disappearance of
481 this alternate hypocortisolic state through compensatory effects of these axes. Only when all
482 three interacting axes were included was an alternate hypocortisolic condition recovered.
483 Therefore while simple models require the inclusion of positive receptor feedback dynamics
484 to produce mutlistability, these effects become inherent in more coarse, but comprehensive
485 regulatory circuits, and receptor-level feedback becomes less of a contributor in the support
486 of multiple attractor states. Coarse-grained but comprehensive models may suffice
487 therefore in capturing physiologically relevant and clinically verifiable response dynamics.
488
489 Our analysis of these coarse grained models spanning across multiple regulatory axes
490 highlighted the important role of gender in supporting a persistent hypocortisolic condition.
491 Due to the suppressive actions of the male gonadal system in regulating itself and the HPA
492 axis, a low cortisol steady state is never available to the male, at least theoretically at this
493 level of detail. In women however, the combined effect of EST and PROG on the HPA still

494 remains somewhat inconsistent [34,63] owing to the varying effects of these hormones
495 during and after the menstrual cycle. EST is generally believed to stimulate the HPA axis
496 during the menstrual cycle [63-65], however evidence indicates that in perimenopausal,
497 menopausal or ovariectomized women the HPA axis response is inversely correlated with
498 plasma EST levels suggesting an inhibitory effect [65,66]. This suggests that sex hormone
499 regulation may change in feedback polarity and act as both inhibitor and activator of the
500 HPA axis. For this reason HPA-HPG interaction in women will in theory readily support the
501 presence of a stable hypocortisolic condition when HPG axis regulation inhibits the HPA axis
502 while stimulating itself.
503
504 In addition to sex hormone regulation, interaction with the immune system also appears to
505 play a significant role in determining abnormal cortisol levels. In our coarse-grain models,
506 cortisol exerts a suppressive action on the innate immune system and the Th1 adaptive
507 immune response. Conversely, positive feedback by certain components of the immune
508 system promotes increases in cortisol levels, which support a hypercortisolic steady state.
509 While, inclusion of the glucocorticoid receptor dimerization (GR-GRD) in these models
510 yielded additional steady states, it did not result in any significant changes to the profile in
511 regards to cortisol levels. Combining the actions of HPA, HPG and immune regulation
512 supported the existence of a stable hypercortisolic state in all models of men and women
513 while a persistent hypocortisolic state was available only in women and only under certain
514 modes of HPG regulation. Once again, while the inclusion of the GR-GRD receptor
515 dimerization in this overarching model yielded additional steady states, it did not result in any
516 significant changes to the homeostatic profiles.
517
518 These findings suggest that abnormally high levels of cortisol and adaptive immune
519 activation, in this case Th1, may be perpetuated under certain conditions by the system's
520 own homeostatic drive. This prediction of persistent and stable Th1 activation is consistent
521 with evidence of anomalies in immune signaling in GWI [55,67,68]. Skowera et al. measured

522 intracellular production of cytokines in peripheral blood and found ongoing Th1-type immune
523 activation in symptomatic Gulf War Veterans compared to healthy counterparts [67]. More
524 recent work confirmed this finding while also suggesting that this may occur in the more
525 complex context of a mixed Th1:Th2 response [55], something not captured by the simple
526 immune model used here. Though we were unable to find documented reports of lower
527 testosterone levels in GWI beyond the experimental data presented here, a large study of
528 gulf war veterans in the UK found increased risk of fertility problems in this population [69],
529 suggesting a possible relation.
530
531 In much the same way, conditions involving hypocortisolism and a Th2 shift may also be
532 perpetuated at least in part by the natural homeostatic regulatory programming. In this case
533 the homeostatic program may be driven by sex steroid suppression of the HPA axis and
534 promotion of HPG function coupled with the mutual inhibition between the Th1 response and
535 function of the gonadal axis, a configuration seemingly available only to female subjects in
536 our models. This would suggest that the hypocortisolism seen in diseases, such as CFS [70-
537 72], could be a result of the complexity afforded by the interaction between the HPA,
538 immune and HPG axes in female subjects. Indeed model predictions describing such an
539 alternate homeostatic state in women aligned with our experimental results from CFS
540 subjects, and is consistent with previous findings of Th2 activation in CFS (Brenu et al.,
541 2011, Nakamura et al., 2010 and Natelson et al., 2005, Broderick et al., 2010). This
542 alignment with a naturally occurring homeostatic conditions may explain, at least in part, the
543 biased prevalence of such persistent diseases in women [73-78]. Indeed, these authors
544 report that approximately 70% of observed CFS patients are women. Additionally, the
545 prevalence of CFS in the 40–49-year-old age range [78], and the higher prevalence of
546 gynecological conditions and gynecological surgeries in women with CFS [79] supports the
547 evidence that HPA suppression by estradiol appears more likely in perimenopausal,
548 menopausal or ovariectomized women [65,66]. Interestingly, as many as 1 in 3 CFS
549 subjects have reported symptom relief during pregnancy [80]. The normal trend in

550 pregnancy towards increased cortisol levels, especially in the third trimester, might be a
551 contributing factor that would support the key involvement of sex hormone regulation
552 proposed by our analysis [81]. While, in normal pregnancy this increase in cortisol typically
553 coincides with an increase in cortisol-binding globulin (CBG) maintaining the level of free
554 cortisol, CBG genetic variants in CFS have the potential to alter normal CBG function
555 [82,83].
556
557 While certainly more comprehensive than their predecessors, these models remain relatively
558 coarse representations of the interplay between the endocrine and immune systems.
559 This is particularly true of immune model granularity, especially when one considers the
560 complex signaling network supported by immune cells as well as other immune-sensitive
561 cells [84]. The important role of key neurotransmitters linking the central nervous system
562 with the HPA axis and the immune system was also under-represented in this first
563 generation of models. For example, norepinephrine and epinephrine stimulate the β_2-
564 adrenoreceptor-cAMP-protein kinase A pathway inhibiting the production of
565 Th1/proinflammatory cytokines and stimulating the production of Th2/anti-inflammatory
566 cytokines causing a selective shift from cellular to humoral immunity [85,86]. Additionally,
567 lymphocytes express most of the cholinergic components found in the nervous system.
568 Lymphocytes may be stimulated by, or release, acetylcholine thus constituting an immune
569 regulating cholinergic system secondary to the nervous system [87]. Another
570 neurotransmitter, neuropeptide Y (NPY), also serves as a powerful immune modulator [88]
571 and has recently been shown to play a role in CFS [89]. These components are without
572 question important, however based on our initial observations from this piecewise analysis
573 we expect that increased detail will lead to the emergence of additional response programs
574 rather than the elimination of attractors found here.
575
576 As these models are based on currently documented knowledge of human physiology and
577 regulatory biochemistry they are necessarily incomplete. Nonetheless the simple models

presented here illustrate the importance of an integrative approach to understanding complex illnesses. Further refinement of the model to include more detailed description of interactions within and between the HPA, HPG and immune systems could extend its applicability to other illnesses as would the incorporation of other key systems such as the brain and central nervous systems. Yet, even with the coarse-grained co-regulation networks investigated we found numerous stable resting states that differ significantly from normal and were indicative of complex and persistent regulatory imbalances. Findings such as this support the use of an alternate model for disease, one which is not necessarily associated with failure of individual components, but rather with a shift in their coordinated actions away from normal regulatory behavior. Response to exercise and other stressors has the potential to be very different in these new regulatory regimes. This is something that we have observed firsthand in our work with human GWI and CFS subjects [90].

Finally, when considering alignment with the experimental data presented here for CFS and GWI, it is important to remember that it was never our hypothesis that these illnesses resulted solely from the actions of homeostatic drive. Instead we proposed that homeostatic drive might be a significant contributor to the persistence of illness mechanisms. Because these naturally occurring regimes, once instantiated, provide an alternate stable homeostasis resistant to change, it may offer fertile ground in support of many chronic pathological processes. The alignment of several immune and endocrine markers modeled here with experimental data from CFS and GWI, two chronic conditions, would support at least partial involvement of the body's own homeostatic drive in facilitating the perpetuation of these conditions. This may promote resistance to therapy and the natural regulatory barrier to change, even positive change, should at least be considered in the design of robust treatment avenues.

Acknowledgments

605 This research was conducted in collaboration with Dr. Joel Zysman, Director of High
606 Performance Computing, using the Pegasus platform at the University of Miami Center for
607 Computational Science (CCS) (http://ccs.miami.edu). This research was also enabled by
608 the use of computing resources provided by WestGrid and Compute/Calcul Canada.
609
610
611 **References**
612

613 1. Groeneweg FL, Karst H, de Kloet ER, Joëls M (2011) Rapid non-genomic effects of
614 corticosteroids and their role in the central stress response. J Endocrinol 209: 153–167.

615 2. Lupien SJ, McEwen BS, Gunnar MR, Heim C (2009) Effects of stress throughout the
616 lifespan on the brain, behaviour and cognition. Nat Rev Neurosci 10: 434-445.

617 3. Mikics É, Kruk MR, Haller J (2004) Genomic and non-genomic effects of glucocorticoids
618 on aggressive behavior in male rats. Psychoneuroendocrino 29: 618–635.

619 4. Pariante CM, Lightman SL (2008) The HPA axis in major depression: classical theories
620 and new developments. Trend Neurosci 31: 464 – 468.

621 5. Gerritsen L, Comijs HC, van der Graaf Y, Knoops AJ, Penninx BW, Geerlings MI (2011)
622 Depression, hypothalamic pituitary adrenal axis, and hippocampal and entorhinal cortex
623 volumes--the SMART Medea study. Biol Psychiatry 70: 373-380.

624 6. Mehta D, Binder EB (2012) Gene × environment vulnerability factors for PTSD: The
625 HPA-axis. Neuropharmacol 62: 654-662.

626 7. Yehuda R (2009) HPA alterations in PTSD. In: Fink G, editor. Stress Consequences:
627 Mental, Neuropsychological and Socioeconomic. San Diego: Academic Press. pp. 125-
628 130.

629 8. Young EA (2009) PTSD and HPA axis: same hormones, different disorders. In: Pariante
630 CM, editor. Understanding Depression: A Translational Approach. New York: Oxford
631 University Press. pp. 193-212.

632 9. Gil-Bea FJ, Aisa B, Solomon A, Solas M, del Carmen Mugueta M, et al. (2010) HPA
633 axis dysregulation associated to apolipoprotein E4 genotype in Alzheimer's disease. J
634 Alzheimers Dis. 22: 829-838.

635 10. Golier JA, Schmeidler J, Legge J, Yehuda R (2006) Enhanced cortisol suppression to
636 dexamethasone associated with Gulf War deployment. Psychoneuroendocrinology
637 31(10): 1181-1189.

638 11. Golier JA, Schmeidler J, Legge J, Yehuda R (2007) Twenty-four hour plasma cortisol
639 and adrenocorticotropic hormone in Gulf War Veterans: relationships to posttraumatic
640 stress disorder and health symptoms. Biol Psychiatry 62(10): 1175–1178.

641 12. Golier JA, Schmeidler J, Yehuda R (2009) Pituitary response to metyrapone in Gulf War
642 veterans: relationship to deployment, PTSD and unexplained health symptoms.
643 Psychoneuroendocrinology 34(9): 1338-1345.

644 13. Van Den Eede F, Moorkens G, Van Houdenhove B, Cosyns P, Claes SJ (2007)
645 Hypothalamic-pituitary-adrenal axis function in chronic fatigue syndrome.
646 Neuropsychobiol 55: 112–120.

647 14. Crofford LJ, Young EA, Engleberg NC, Korszun A, Brucksch CB, et al. (2004) Basal
648 circadian and pulsatile ACTH and cortisol secretion in patients with fibromyalgia and/or
649 chronic fatigue syndrome. Brain Behav Immun 18: 314–325.

650 15. Aschbacher K, Adam EK, Crofford LJ, Kemeny ME, Demitrack MA, et al. (2012) Linking
651 disease symptoms and subtypes with personalized systems-based phenotypes: A proof
652 of concept study. Brain Behav Immun. 26(7):1047-1056..

16. Ben-Zvi A, Vernon SD, Broderick G (2009) Model-Based Therapeutic Correction of Hypothalamic-Pituitary-Adrenal Axis Dysfunction. PLoS Comp Biol 5: e1000273.

17. Alon U. Network motifs: theory and experimental approaches. Nat Rev Genet. 2007 Jun;8(6):450-61. Review.

18. Lightman SL, Conway-Campbell BL (2010) The crucial role of pulsatile activity of the HPA axis for continuous dynamic equilibration, Nat Rev Neurosci 11: 710-718.

19. Bairagi N, Chatterjee S, Chattopadhyay J (2008) Variability in the secretion of corticotropin-releasing hormone, adrenocorticotropic hormone and cortisol and understandability of the hypothalamicpituitary-adrenal axis dynamics--a mathematical study based on clinical evidence. Math Med Biol 25: 37–63.

20. Kyrylov V, Severyanova LA, Vieira A (2005) Modeling robust oscillatory behavior of the hypothalamic-pituitary-adrenal axis. IEEE Trans Biomed Eng 52: 1977–1983.

21. Savic D, Jelic S (2005) A theoretical study of hypothalamo-pituitary adrenocortical axis dynamics. Ann NY Acad Sci 1048: 430–432.

22. Savic D, Jelic S (2005) A mathematical model of the hypothalamopituitary-adrenocortical system and its stability analysis. Chaos Solitons Fractals 26: 427–436.

23. Lenbury Y, Pornsawad P (2005) A delay-differential equation model of the feedback-controlled hypothalamus-pituitary-adrenal axis in humans. Math Med Biol 22: 15–33.

24. Gonzalez-Heydrich J, Steingard RJ, Kohane I (1994) A computer simulation of the hypothalamic-pituitary-adrenal axis. Proc Annu Symp Comput Appl Med Care 1994: 1010.

25. Dempsher DP, Gann DS, Phair RD (1984) A mechanistic model of ACTH-stimulated cortisol secretion. Am J Physiol 246: R587-R596.

676 26. Sharma DC, Gabrilove JL (1975) A study of the adrenocortical disorders related to the
677 biosynthesis and regulation of steroid hormones and their computer simulation. Mt Sinai
678 J Med 42: S2-S39.

679 27. Gupta S, Aslakson E, Gurbaxani BM, Vernon SD (2007) Inclusion of the glucocorticoid
680 receptor in a hypothalamic pituitary adrenal axis model reveals bistability. Theor Biol
681 Med Model 4: 8.

682 28. Alon U (2007) Network motifs: theory and experimental approaches. Nat Rev Genet 8:
683 450-461.

684 29. Thomas R, Thieffry D, Kaufman M (1995) Dynamical behaviour of biological regulatory
685 networks--I. Biological role of feedback loops and practical use of the concept of the
686 loop-characteristic state. Bull Math Biol. 57: 247-276.

687 30. Thomas R (1991) Regulatory Networks Seen as Asynchronous Automata: A Logical
688 Description. J Theor Biol 153: 1-23.

689 31. Mendoza L, Xenarios I (2006) A method for the generation of standardized qualitative
690 dynamical systems of regulatory networks Theor Biol Med Model 3: 13.

691 32. Keller-Wood ME, Dallman MF (1984) Corticosteroid inhibition of ACTH secretion.
692 Endocrinol Rev 5: 1–24.

693 33. Viau V (2002) Functional Cross-Talk Between the Hypothalamic-Pituitary-Gonadal and -
694 Adrenal Axes. J Neuroendocrinol 14: 506–513.

695 34. Dallman MF, Viau V, Bhatnagar S, Laugero K, Gomez F, et al. (2002) Corticotropin-
696 releasing factor (CRF), corticosteroids and stress, energy balance, the brain and
697 behavior. In: Pfaff DW, editor. Hormones, Brain and Behavior. New York: Academic
698 Press. Pp. 571-632.

699 35. Tilbrook AJ, Turner AI, Clarke IJ (2000) Effects of stress on reproduction in non-rodent
700 mammals: the role of glucocorticoids and sex differences. Rev Reprod 5: 105–113.

701 36. Torpy DJ, Chrousos GR (1996) The three-way interactions between the hypothalamic-
702 pituitary-adrenal and gonadal axes and the immune system. Baillires Clin Rheumatol
703 10: 181-198.

704 37. Rivier C, Rivest S (1991) Effect of stress on the activity of the hypothalamic pituitary-
705 gonadal axis: peripheral and central mechanisms. Biol Reprod 45: 523–532.

706 38. Piñón R (2001) Biology of human reproduction. Sausalito: University Science Books.
707 535 p.

708 39. Hiller-Sturmhöfel S, Bartke A (1998) The endocrine system: an overview. Alcohol Health
709 Res World 22:153-164.

710 40. Folcik VA, Broderick G, Mohan S, Block B, Ekbote C, Doolittle J et al. (2011) Using an
711 agent-based model to analyze the dynamic communication network of the immune
712 response. Theor Biol Med Model 8: 1.

713 41. Silverman MN, Pearce BD, Biron CA, Miller AH (2005) Immune modulation of the
714 hypothalamic-pituitary-adrenal (HPA) axis during viral infection. Viral Immunol 18: 41-
715 78.

716 42. Cutolo M (2004) Immune System, Hormonal Effects on. In: Martini L, editor.
717 Encyclopedia of Endocrine Diseases, Volume 2. Elsevier Academic Press. pp. 755-760.

718 43. Berczi I, Szentivanyi A (2003) Autoimmune disease. In: Berczi I, Szentivanyi A, editors.
719 Neuroimmmune Biology: Vol. 3: The Immune-Neuroendocrine Circuitry. History and
720 Progress. Amsterdam: Elsevier Science BV. pp. 495-536

721 44. Bush KA, Krukowski K, Eddy JL, Janusek LW, Mathews HL (2012) Glucocorticoid
722 receptor mediated suppression of natural killer cell activity: Identification of associated
723 deacetylase and corepressor molecules. Cell Immunol 275:80-89.

724 45. Zen M, Canova M, Campana C, Bettio S, Nalotta L, et al. (2011) The kaleidoscope of
725 glucocorticoid effects on immune system. Autoimmun Rev 10: 305-310.

726 46. Liberman AC, Druker J, Refojo D, Holsboer F, Arzt E (2009) Glucocorticoids inhibit
727 GATA-3 phosphorylation and activity in T cells. FASEB J 23: 1558-1571.

728 47. Elenkov IJ (2004) Glucocorticoids and the Th1/Th2 balance. Ann NY Acad Sci 1024:
729 138-146.

730 48. González D, Díaz B, Pérez M, Hernández A, Chico B, et al. (2010) Sex hormones and
731 autoimmunity. Immunol Lett 133: 6-13.

732 49. Lélu K, Laffont S, Delpy L, Paulet PE, Périnat T et al. (2011) Estrogen Receptor α
733 Signaling in T Lymphocytes Is Required for Estradiol-Mediated Inhibition of Th1 and
734 Th17 Cell Differentiation and Protection against Experimental Autoimmune
735 Encephalomyelitis. J Immunol 187: 2386-2393.

736 50. Foster S, Daniels C, Bourdette D, Bebo BF (2003) Dysregulation of the hypothalamic
737 pituitary-gonadal axis in experimental autoimmune encephalomyelitis and multiple
738 sclerosis. J Neuroimmunol 140: 78-87.

739 51. Watanobe H, Hayakawa Y (2003) Hypothalamic interleukin-1 beta and tumor necrosis
740 factor-alpha, but not interleukin-6, mediate the endotoxin-induced suppression of the
741 reproductive axis in rats. Endocrinology 144: 4868-4875.

742 52. Fukuda K, Nisenbaum R, Stewart G, Thompson WW, Robin L, et al. (1998) Chronic
743 multisymptom illness affecting Air Force veterans of the Gulf War. J Am Med Assoc 280:
744 981–998.

745 53. Fukuda, K., Straus, S.E., Hickie, I., Sharpe, M.C., Dobbins, J.G., Komaroff, A., 1994.
746 The chronic fatigue syndrome: a comprehensive approach to its definition and study.
747 International Chronic Fatigue Syndrome Study Group. Ann. Intern. Med. 12, 953-959.

748 54. Collins JF, Donta ST, Engel CC, Baseman JB, Dever LL, et al. (2002) The antibiotic
749 treatment trial of Gulf War Veterans' Illnesses: issues, design, screening, and baseline
750 characteristics. Control Clin Trials 23: 333–353.

751 55. Broderick G, Kreitz A, Fuite J, Fletcher MA, Vernon SD, et al. (2011) A pilot study of
752 immune network remodeling under challenge in Gulf War Illness. Brain Behav Immun
753 25: 302–313.

754 56. Vernon SD, Reeves WC (2006) The challenge of integrating disparate high-content
755 data: epidemiological, clinical and laboratory data collected during an in-hospital study
756 of chronic fatigue syndrome. Pharmacogenomics 7: 345–354.

757 57. Fuite J, Vernon SD, Broderick G (2008) Neuroendocrine and immune network re-
758 modeling in chronic fatigue syndrome: An exploratory analysis. Genomics 92: 393–399.

759 58. Broderick G, Craddock RC, Whistler T, Taylor R, Klimas N, et al. (2006) Identifying
760 illness parameters in fatiguing syndromes using classical projection methods.
761 Pharmacogenomics 7: 407–419.

762 59. Broderick G, Fuite J, Kreitz A, Vernon SD, Klimas N, et al. (2010) A formal analysis of
763 cytokine networks in Chronic Fatigue Syndrome. Brain Behav Immun 24: 1209-1217.

764 60. Reeves WC, Lloyd A, Vernon SD, Klimas N, Jason LA, et al. (2003) Identification of
765 ambiguities in the 1994 chronic fatigue syndrome research case definition and
766 recommendations for resolution. BMC Health Serv Res 3: 25.

767 61. Brown M (1975) A method for combining non-independent, one-sided tests of
768 significance. Biometrics 31: 987–992.

769 62. Beacher FDCC, Gray MA, Mathias CJ, Crichlek HD (2009) Vulnerability to simple faints
770 is predicted by regional differences in brain anatomy, NeuroImage 47: 937-945.

771 63. Wolfram M, Bellingrath S, Kudielka BM (2011) The cortisol awakening response (CAR)
772 across the female menstrual cycle. Psychoneuroendocrinol 36: 905-912.

773 64. Chrousos GP (2010) Stress and Sex Versus Immunity and Inflammation. Sci Signal 3:
774 pe36

775 65. Young EA, Korszun A, Figueiredo HF, Banks-Solomon M, Herman JP (2007) Sex
776 Differences in HPA axis regulation, In: Becker JB, Berkley KJ, Geary N, Hampson E,
777 Herman JP, et al., editors. Sex Differences in the Brain: From Genes to Behavior. New
778 York, USA: Oxford University Press. pp. 95-105.

779 66. Tarín JJ, Hamatani T, Cano A (2010) Acute stress may induce ovulation in women.
780 Reprod Biol Endocrinol 8: 53.

781 67. Skowera A, Hotopf M, Sawicka E, Varela-Calvino R, Unwin C et al. (2004) Cellular
782 Immune Activation in Gulf War Veterans. J Clin Immunol 24: 66-73.

783 68. Whistler T, Fletcher MA, Lonergan W, Zeng XR, Lin JM, et al. (2009) Impaired immune
784 function in Gulf War Illness. BMC Medical Genomics 2: 12.

785 69. Doyle P, Maconochie N, Ryan M (2006) Reproductive health of Gulf War veterans.
786 Philos Trans R Soc Lond B Biol Sci 361:571-584.

787 70. Papadopoulos AS, Cleare AJ (2012) Hypothalamic–pituitary–adrenal axis dysfunction in
788 chronic fatigue syndrome. Nat Rev Endocrinol 8: 22-32

789 71. Jerjes WK, Peters TJ, Taylor NF, Wood PJ, Wessely S, et al. (2006) Diurnal excretion of
790 urinary cortisol, cortisone, and cortisol metabolites in chronic fatigue syndrome.
791 Psychosom Res 60: 145–153.

792 72. Cleare AJ (2003) The neuroendocrinology of chronic fatigue syndrome. Endocr Rev 24:
793 236–252.

794 73. Nacul LC, Lacerda EM, Pheby D, Campion P, Molokhia M, et al. (2011) Prevalence of
795 myalgic encephalomyelitis/chronic fatigue syndrome (ME/CFS) in three regions of
796 England: a repeated cross-sectional study in primary care. BMC Med 9: 91.

797 74. Evengard B, Jacks A, Pedersen N, Sullivan PF (2005) The epidemiology of chronic
798 fatigue in the Swedish Twin Registry. Psych Med 35: 1317-1326.

799 75. Gallagher AM, Thomas JM, Hamilton WT, White PD (2004) Incidence of fatigue
800 symptoms and diagnoses presenting in UK family care from 1990 to 2001. J Roy Soc
801 Med 97: 571-575.

802 76. Reyes M, Nisenbaum R, Hoaglin D, Unger ER, Emmons C, et al. (2003) Prevalence
803 and incidence of chronic fatigue syndrome in Wichita, Kansas. Arch Intern Med 163:
804 1530-1536.

805 77. Lindal E, Stefansson JG, Bergmann S (2002) The prevalence of chronic fatigue
806 syndrome in Iceland—a national comparison by gender drawing on four different
807 criteria. Nord J Psychiatry 56: 273-277. Erratum in: Lindal E, Stefansson JG, Bergmann
808 S (2006) Nord J Psychiatry. 60: 183.

809 78. Jason LA, Richman JA, Rademaker AW, Jordan KM, Plioplys AV, et al. (1999) A
810 community-based study of chronic fatigue syndrome. Arch Intern Med 159: 2129-2137.

811 79. Boneva RS, Maloney EM, Lin JM, Jones JF, Wieser F, et al. (2011) Gynecological
812 History in Chronic Fatigue Syndrome: A Population-Based Case-Control Study. J
813 Womens Health 20: 21-28.

814 80. Schacterle RS, Komaroff AL (2004) A comparison of pregnancies that occur before and
815 after the onset of chronic fatigue syndrome. Arch Intern Med 164:401-404.

816 81. Gangestad SW, Caldwell Hooper AE, Eaton MA (2012) On the function of placental
817 corticotropin-releasing hormone: a role in maternal-fetal conflicts over blood glucose
818 concentrations. Biol Rev Camb Philos Soc 87:856-873.

819 82. Torpy DJ, Ho JT (2007) Corticosteroid-binding globulin gene polymorphisms: clinical
820 implications and links to idiopathic chronic fatigue disorders. Clin Endocrinol (Oxf)
821 67:161-167.

822 83. Gagliardi L, Ho JT, Torpy DJ (2010) Corticosteroid-binding globulin: the clinical
823 significance of altered levels and heritable mutations. Mol Cell Endocrinol 316: 24-34.

824 84. Frankenstein Z, Alon U, Cohen IR (2006) The immune-body cytokine network defines a
825 social architecture of cell interactions. Biol Direct 1: 32.

826 85. Kin NW, Sanders VM (2006) It takes nerve to tell T and B cells what to do. J Leukocy
827 Biol 79: 1093-1104.

828 86. Elenkov IJ, Wilder RL, Chrousos GP, Vizi ES (2000) The Sympathetic Nerve—An
829 Integrative Interface between Two Supersystems: The Brain and the Immune System.
830 Pharmacol Rev 52: 595-638.

831 87. Kawashima K, Fujii T (2003) The lymphocytic cholinergic system and its contribution to
832 the regulation of immune activity. Life Sci 74: 675–696.

833 88. Wheway J, Mackay CR, Newton RA, Sainsbury A, Boey D, Herzog H, Mackay F (2005)
834 A fundamental bimodal role for neuropeptide Y1 receptor in the immune system. J Exp
835 Med 202:1527-1538.

836 89. Fletcher MA, Rosenthal M, Antoni M, Ironson G, Zeng XR, et al. (2010). Plasma
837 neuropeptide Y: a biomarker for symptom severity in chronic fatigue syndrome. Behav
838 Brain Funct. 6: 76.

90. Broderick G, Fletcher MA, Gallgher M, Barnes Z, Vernon SD, et al. (2012) Exploring the Predictive Potential of Immune Response to Exercise in Gulf War Illness. In: Yan Q. (Ed.), Psychoneuroimmunology: Methods and Protocols (Methods in Molecular Biology), Springer, New York, NY, In Press

Tables

Table 1: Ternary HIGH/LOW PASS operator

A ∇B	B = -1	B = 0	B = 1
A = -1	0	0	-1
A = 0	0	0	-1
A = 1	1	1	0

Table 2: Ternary OR operator

A∨B	B = -1	B = 0	B = 1
A = -1	-1	0	1
A = 0	0	0	1
A = 1	1	1	1

Table 3: Ternary NOT operator

A	¬ A
-1	1
0	0
1	-1

Figure Legends

Figure 1: Standard and extended HPA models. (A) Standard HPA model. (B) HPA-GR model of Gupta et al. [27]. Integrated models (C) HPA-GR-Immune-HPGa for males, and (D) HPA-GR-Immune-HPGb, (E) HPA-GR-Immune-HPGc, (F) HPA-GR-Immune-HPGd, and (G) HPA-GR-Immune-HPGe for females.

Figure 2: Steady states of standard and extended HPA models. White – nominal state (0); Green – high state (1); Red – low state (-1); Grey – N/A to the model.

Figure 1

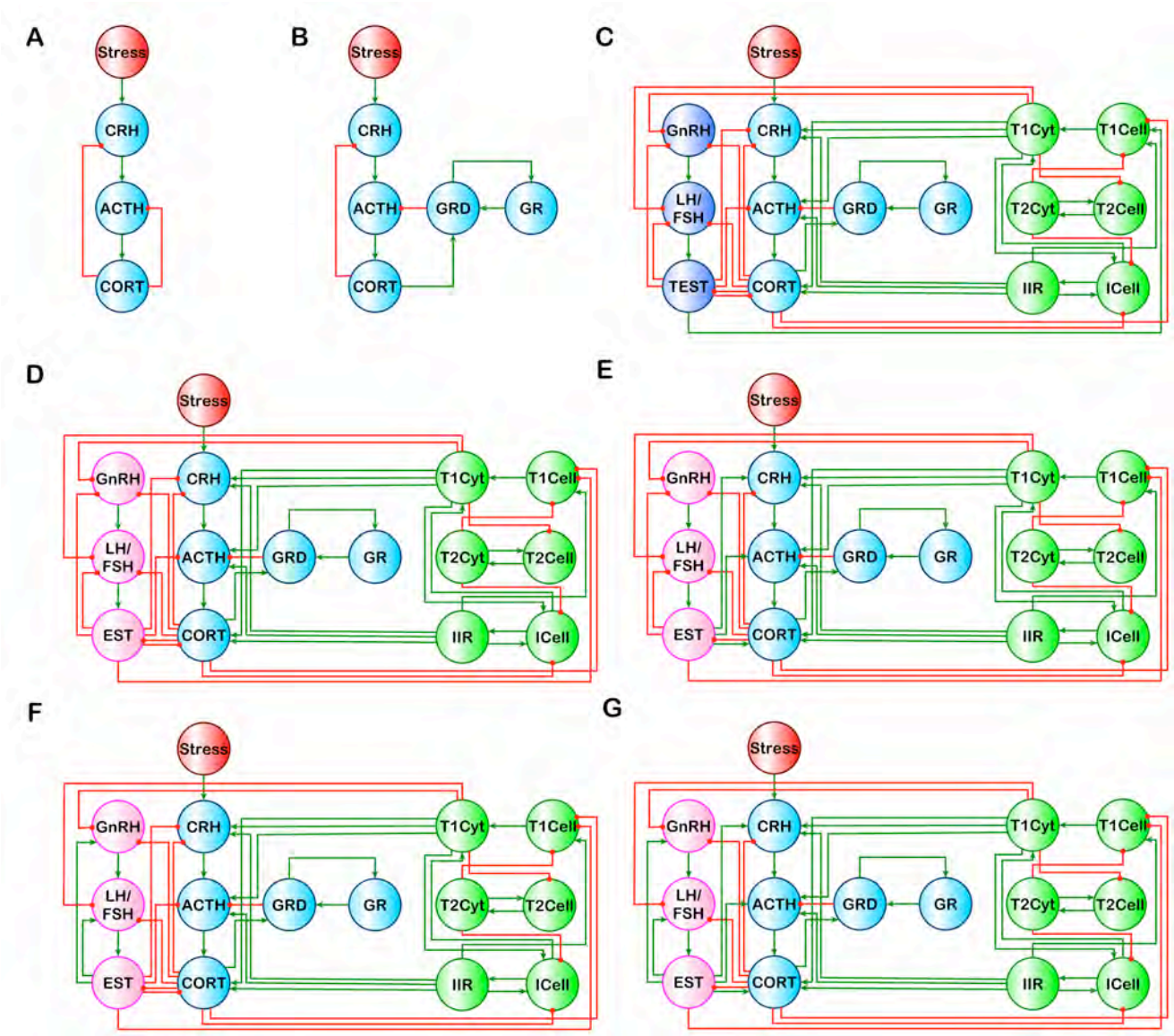
A
Stress
CRH
ACTH
CORT
B
Stress
CRH
ACTH
GRD
GR
CORT
C
Stress
GnRH
CRH
T1Cyt
T1Cell
LH/
FSH
ACTH
GRD
GR
T2Cyt
T2Cell
TEST
CORT
IIR
ICell
D
Stress
GnRH
CRH
T1Cyt
T1Cell
LH/
FSH
ACTH
GRD
GR
T2Cyt
T2Cell
EST
CORT
IIR
ICell
E
Stress
GnRH
CRH
T1Cyt
T1Cell
LH/
FSH
ACTH
GRD
GR
T2Cyt
T2Cell
EST
CORT
IIR
ICell
F
Stress
GnRH
CRH
T1Cyt
T1Cell
LH/
FSH
ACTH
GRD
GR
T2Cyt
T2Cell
EST
CORT
IIR
ICell
G
Stress
GnRH
CRH
T1Cyt
T1Cell
LH/
FSH
ACTH
GRD
GR
T2Cyt
T2Cell
EST
CORT
IIR
ICell

Figure 2

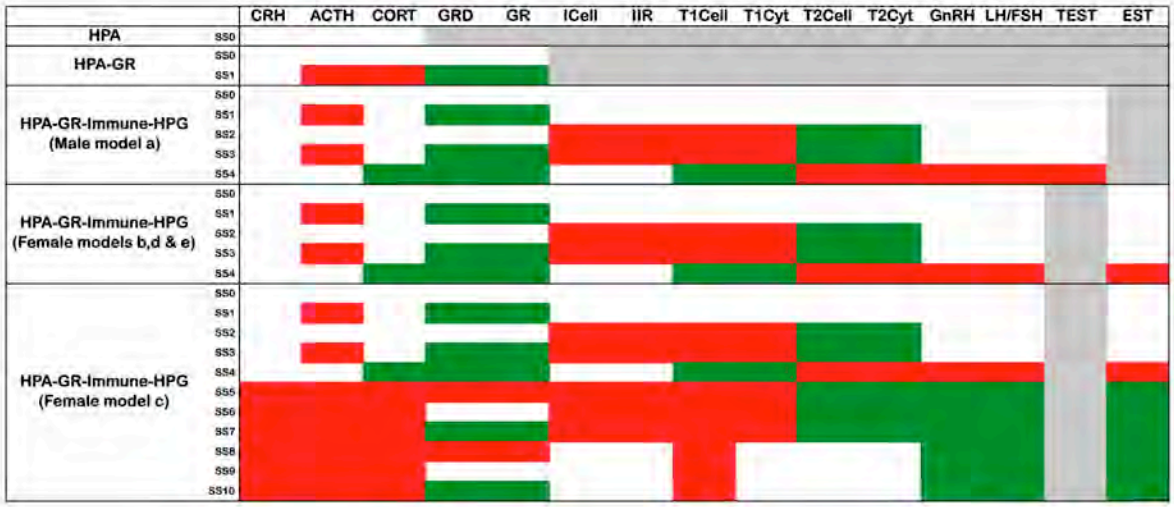
CRH
ACTH
CORT
GRD
GR
ICell
IIR
T1Cell
T1Cyt
T2Cell
T2Cyt
GnRH
LH/FSH
TEST
EST
HPA
SS0
HPA-GR
SS0
SS1
HPA-GR-Immune-HPG
(Male model a)
SS0
SS1
SS2
SS3
SS4
HPA-GR-Immune-HPG
(Female models b,d & e)
SS0
SS1
SS2
SS3
SS4
HPA-GR-Immune-HPG
(Female model c)
SS0
SS1
SS2
SS3
SS4
SS5
SS6
SS7
SS8
SS9
SS10

Appendix B:

Updated scope of work (SOW) submitted as part of request for transition of award to Nova Southeastern University.

Revised Statement of Work (SOW) - Relocation to Nova Southeastern University (NSU), FL

The following SOW has been updated to reflect current status of project consistent with the annual progress report submitted in September, 2012. Described are the remaining activities required for completion. These will now be conducted by the Broderick group from its new home institution: Nova Southeastern University, Fort Lauderdale, Florida.

In support of Dr. Broderick's transition Nova Southeastern University is entering into a service agreement with the Center for Computational Sciences (CCS) at the University of Miami, which will serve as the principal high-performance computing resource for the Broderick group from this point forward. The latter will continue to use the University of Alberta's WestGrid high-performance computing platform during the transition period in order to ensure continuity of the work.

Task 1. *Evaluate and select agent-based simulation environment*. **Completed**.

Task 2. *Define and encode immune cell populations and interaction rules*. **Completed**.

Task 3. *Refine HPA axis model and integrate with immune model*. **Completed**.

MILESTONE I: Completion and release of validated model combining ODE representation of the HPA axis and a discrete population-based model of the immune system. Target date: **Completed**.

Extensions to original Task 2, 3.

3.a. *Extension of circuit model of neuro-inflammatory cascades.* In an extension of the original mandate for Task 2, the circuit logic approach is also being applied to model inflammatory processes occurring in the brain and involving the cell types and immune signaling specific to this physiological compartment.

3.b. *Extension to sex hormone and thyroid axes.* Task 3 has also been extended beyond the original mandated scope to now include the endocrine axis regulating sex hormones. We expect to integrate thyroid function in this regulatory circuitry as well.

Timeline extended mandate: Months 1-4, Year 3 (now December, 2013)
Site(s): Nova Southeastern University

Task 4. *Design and conduct formal sensitivity and multi-stability analyses*. **Completed**

Task 5. *Network analysis of alternate homeostatic states*. **Completed**

Extensions to original Task 4, 5. These steps will be repeated in the analysis of the extensions to the model proposed in 3(a) and 3(b).

Timeline extended mandate: Months 1-4, Year 3 (now December, 2013)
Site(s): Nova Southeastern University

MILESTONE II: Verification of hypothesis that GWI symptoms persist because the endocrine-immune system now occupies and alternate homeostatic stable point and engages a new sub-optimal stress response control program.
Target date: Month 4, Year 3 (now December, 2013); Currently 70% complete.

Task 6. *Identify and deploy large-scale optimization*. This involves the selection of the best algorithm for exhaustive search of intervention possibilities. We expect the combined endocrine-immune system to present multiple stable points and the landscape describing its dynamic response to be complex. As a result standard techniques for optimization of treatment time course would terminate their search in the first region where treatment performance ceases to improve. Overall such a treatment may be quite remote from that available in the neighboring response "valley".
Timeline: Months 2-4, Year 3 (now October - December 2013)

6.a. *Review global search algorithms*. Review latest developments in evolutionary programming techniques as well as hybrid techniques to determine the most suitable search algorithm. Acquire or develop code and deploy on CCS platform and test on logic model developed in 4b.
Timeline: Month 1-2, Year 3 (now September - October 2013)
Site(s): Nova Southeastern University

6.b. *Configure simulation-based optimization scheme*. Configure an interface that evaluates the fitness of candidate interventions by repeatedly launching short logic model simulations as it conducts its search for the most robust treatment course. Test and deploy.
Timeline: Months 2-6, Year 3 (now October - February, 2014)

Site(s): Nova Southeastern University

Task 7. *Identify candidate treatment courses for GWI.* Using the optimization scheme developed and deployed in Task 6, launch optimization runs from multiple initial conditions of endocrine-immune status. Assess these options and report.

Timeline: Months 5-12 Year 3

7.a. *Define and encode solution fitness criteria*. Identify and describe mathematically the immune and endocrine descriptors that can be safely changed and over what range they may be changed. Incorporate these constraints with treatment goals and define optimization problem formally.
Timeline: Month 3-5, Year 3 (now November, 2013 - January, 2014)
Site(s): Nova Southeastern University

7.b. *Search for broadly applicable candidate treatment courses*. Identify a set of initial conditions of cytokine, hormone and immune cell abundance and launch repeated searches for optimal treatments from these points.
Timeline: Months 6-9, Year 3 (now February - May, 2014)
Site(s): Nova Southeastern University

7.c. *Critically assess candidate treatments.* Review candidate treatment courses and assess these critically based on efficacy and minimal invasiveness. Propose design of pilot clinical trials for evaluation of the best candidates.
Timeline: Months 10-11, Year 3 (now June - July, 2014)
Site(s): Nova Southeastern University

7.d. *End of project review and report*. Timeline: Month 12, year 3 (now August, 2014).